Published in final edited form as:
Hear Res. 2010 January ; 259(1-2): 1. doi:10.1016/j.heares.2009.06.004.

Response Properties of Cochlear Nucleus Neurons in Monkeys

William S. Rhode,
Department of Physiology, University of Wisconsin, 1300 University Avenue, Madison, WI 53706, USA, rhode@physiology.wisc.edu, Phone: +1-608-262-7953, Fax: +1-608-265-5512

G. Linn Roth, and
Department of Physiology, University of Wisconsin, 1300 University Avenue, Madison, WI 53706, USA, rothlinn@sbcglobal.net

A. Recio
Department of Physiology, University of Wisconsin, 1300 University Avenue, Madison, WI 53706, USA, a.recio@lumc.nl

Abstract

Much of what is known about how the cochlear nuclei participate in mammalian hearing comes from studies of non-primate mammalian species. To determine to what extent the cochlear nuclei of primates resemble those of other mammalian orders, we have recorded responses to sound in three primate species: marmosets, Cynomolgus macaques, and squirrel monkeys. These recordings show that the same types of temporal firing patterns are found in primates that have been described in other mammals. Responses to tones of neurons in the ventral cochlear nucleus have similar tuning, latencies, post-stimulus time and interspike interval histograms as those recorded in non-primate cochlear nucleus neurons. In the dorsal cochlear nucleus, too, responses were similar. From these results it is evident that insights gained from non-primate studies can be applied to the peripheral auditory system of primates.

Keywords

Primates; Response properties; Cochlear nucleus; Auditory system

1. Introduction

Differences in the dendritic morphology, axonal projections, convergence of inputs from the auditory nerve and from excitatory and inhibitory interneurons, and intrinsic biophysical characteristics cause neurons in the cochlear nuclear (CN) complex to have distinctive responses to sound in non-primate mammalian species (for reviews, see Young and Oertel, 2004; Rhode and Greenberg, 1992). In primates, responses to sound have been recorded but

Correspondence to: William S. Rhode.

Present addresses. Alberto Recio-Spinoso, ENT Department, Leiden University Medical Center, Postbus 9600, 2300 RC Leiden, Netherlands, a.recio@lumc.nl
Linn Roth, 118 Vaughn Court, Madison, WI 53705, rothlinn@sbcglobal.net

correlations between anatomical and functional properties have not yet been made (Ryan et al., 1984).

Anatomical differences are more obvious in the dorsal (DCN) than in the ventral (VCN) subdivision of the cochlear nucleus in primates and non-primate mammals. From non-primate mammals to monkeys to man, there is a progressive: 1) reduction in the number of granular cells in the CN complex; 2) movement of DCN fusiform (also termed bipolar or pyramidal) cells to more central regions of that CN subdivision; 3) decrease of the associated granular – fusiform cell lamination in the DCN; and 4) loss of the granular layer over the AVCN and PVCN (Fuse, 1913; Moskowitz, 1969; Dublin, 1976; Moore and Osen, 1979a,b; Moore, 1980; Heiman-Patterson and Strominger, 1985). However, a recent study on the rhesus macaque indicates that the primate DCN does contain a granule cell architecture appropriate to perform the integration of acoustic and somatosensory input used by non-primates to orient to sounds and argues that the neuronal features of the primate and non-primate DCN are similar (Rubio et al., 2008). In the VCN of primates the same anatomical cell types are found as in other mammals. Bushy cells are most common anteriorly while multipolar cells and octopus cells are most common posteriorly (Adams, 1986; Adams, 1997).

Given the anatomical similarities and differences, the question arises whether response patterns of anatomically defined cells in the non-primate CN are also present in the primate. In non-primate studies, peristimulus time histograms (PSTHs) and interspike interval histograms (ISIHs) produced by suprathreshold, short tone bursts at characteristic frequency (CF) provide the basis for categorizing a neuron's physiologic response. The response types have been correlated with anatomical cell types by reconstructing electrode paths and by intracellular labeling. Sustained chopper (Cs) and transient chopper (Ct) units have been associated with multipolar (stellate) cells in the AVCN and PVCN, primary-like (PL) and primary-like with notch (PLn) units with small and large spherical and globular/bushy cells in the AVCN, onset-ideal (OnI) and onset-chopper (OnC) units with octopus and multipolar cells in the PVCN (Rhode et al., 1983a; Smith and Rhode, 1989; Palmer et al., 2003; Joris et al., 1994a,b), and pauser (P), buildup (B), and wide chopper (Cw) units with pyramidal (fusiform) cells in the DCN (Rhode et al., 1983a,b; Roullier and Ryugo, 1984; Smith and Rhode, 1985, [1987], 1989; Oertel et al., 1988; Arnott et al., 2004; Hancock and Voigt, 2002).

Here we describe how cochlear nuclear neurons respond to tone bursts and amplitude modulated signals in two New-world monkey (i.e. marmoset and squirrel monkey) and one Old-world monkey (i.e. Cynomolgus macaque) species. Data are reported from one marmoset, seven squirrel monkeys, and three macaques. These data establish a foundation to begin the evaluation of the similarities and differences between response properties of CN neurons in primate and non-primate species and the assessment of what those similarities and differences might mean.

2. Methods

2.1. Surgical preparation

Three Cynomolgus macaques were studied in July and November of 2001 and June of 2004; seven squirrel monkeys were studied from December 2003 through March 2004; and one marmoset was studied in January 2005. Experiments performed were based on animal availability and cost with the goal of comparing cat and monkey cochlear nucleus data. Macaques were non-naïve animals donated by a drug company and appeared to have somewhat higher thresholds than expected. Monkeys ranged in size from approximately 700 grams (Squirrel monkeys) to 5 kilograms (Cynomolgus macaques). Initial induction of anesthesia was achieved by administration of Ketamine (8–10 mg/Kg, IM). Then an initial dose of pentobarbital (10–15 mg/Kg, IV) was followed by additional smaller doses (5–10 mg/Kg, IV)

to maintain the animal in a deeply areflexive state in accordance with NIH guidelines. All procedures were approved by the Animal Care and Use Committee of the University of Wisconsin.

After opening the skull, portions of the cortex and cerebellum were aspirated to expose the CN complex. An outline of the CN was sketched, and locations of penetrations were recorded on the sketch. A plastic chamber was cemented over the opening in the skull, and a 2% agar solution dripped over the CN. Warmed mineral oil was used to fill the chamber, and a glass cover was sealed to the top of the chamber with high vacuum grease to create a hydraulic seal and reduce pulsations. Recordings were made using low impedance (10–20 Mohm) micropipettes filled with 1M KCl, and a hydraulic microdrive was used to advance the electrodes remotely. While the entire CN complex was sampled, the focus of this study was on the VCN.

At the end of a recording session, the animal was euthanized with pentobarbital. Some animals were perfused through the heart with 1 liter 10% formalin. The brain was removed and a cross-section of the brainstem containing the CN was cut and placed in 10% formalin overnight. Histological verification of electrode position and electrode tracks was not possible because the micropipettes did not result in sufficient gliosis to detect the track with a cresyl-violet stain.

2.2. Reconstruction of Penetrations

Each electrode penetration was reconstructed to provide a rough estimate of the location of each studied neuron and to document the progression of CFs and cell types within the CN. Unit depth (dorsal-to-ventral) below the pial surface was plotted as a function of CF, and the classification of each isolated unit was then added. These plots were used to estimate unit location within the CN complex. However, because of the limited number of animals and typically small number of penetrations in each, a more comprehensive histological verification was not practical. Typically, mm scales were placed in the coronal and parasaggital planes during each experiment so that it was fairly certain when the VCN was being studied. The nimianl electrode location was then checked against cresyl-violet sections of the CN that were available for each species.

2.3. Stimulus generation/presentation and response measures

Auditory stimuli were generated on a digital stimulus system that had a 16-bit D/A with a 500 kHz clock rate and timed unit firing to 1 μs precision (Olson et al., 1985). Prior to data collection, a Radio Shack super tweeter was calibrated with a 1/2 inch Brüel & Kjaer condenser microphone/probe tube combination between 100 and 30,000 Hz in 100 Hz steps, and the stimulus system compensated for that calibration. The speaker was housed in a small aluminum case and coupled to the ear canal with plastic tubing. Calibration was performed in the ear canal with the tip of the probe tube near the tympanic membrane. The distance from the probe to the eardrum varied with the different species.

The exception to the above description was stimulus calibration in the macaque because of anatomical constraints, i.e. this species has a very narrow (~2mm) and long (>1.5 cm) earcanal with a very small space in front of the tympanic membrane, which prevented placement of the probe microphone near the tympanic membrane. Here, intensities at the eardrum were estimated by placing the probe tube in front of the opening to the ear canal (i.e. macaque anatomy makes is necessary to use a nearly free field stimulus). As a result, it is possible that the reported thresholds could easily be off by 20 dB SPL, and this calibration issue could account for at least part of the higher unit thresholds that were found in this species.

Auditory units were identified using a tone continuously swept from 0.1 – 30 kHz every 2 s. Responses to swept frequencies enabled an initial estimate of each unit's characteristic frequency (CF). For each unit that was well discriminated, responses to sounds were characterized using the following paradigms: (a) the response area (RA) was determined using 50 ms tone pips presented every 200 ms with the intensity varied from 0 to 90 dB SPL in 10 dB increments. Frequency was varied in CF/10 to CF/20 Hz steps, and 5 repetitions of each stimulus were presented. For all tone pip stimuli, the rise/fall time was 3 ms (cosine); (b) the PSTH at CF was generated using 250 repetitions of a 50 ms tone presented every 200 ms at 60 dB SPL unless otherwise noted; (c) a rate curve (RC) was established at CF over approximately a 90 dB range in 5 dB steps using 50 ms tones presented 10 times every 300 ms; (d) an FM sweep response at a single intensity (~70 dB SPL) was collected; and (e) an amplitude modulated (AM) signal was presented to determine the temporal modulation transfer function (MTF; see Rhode and Greenberg, 1994). The AM carrier was set to CF and the modulation was 100%, 100 ms duration, repeated every 200 ms, 10 times at stimulus intensities of 30, 50, and 70 dB SPL or 50, 70, and 90 dB SPL. The modulation frequency was usually presented in 100 Hz steps between 50 or 100 and 2550 Hz. Occasionally, digitally synthesized white wide-band noise was used to derive a rate curve. The entire stimulus series was rarely completed.

The response properties, nomenclature, and computational methods used were as follows: Response areas: the method of stimulus presentation is described above, and RA spike rates were generated using a 50 ms analysis window. RA data were smoothed with a 3-point moving average using the "filtfilt.m" function in MATLAB (see below). In order to provide tuning curve and RA information in a single illustration, color coded response maps are used, and each associated reference bar indicates spike rates for the unit. However, using response maps often does not illustrate inhibitory side bands well, because those small decreases in rate are not apparent in subtle color changes. When inhibitory side bands were observed for a unit using a standard iso-intensity response area graph, it is stated in the text.

Spontaneous rate and dynamic range: spontaneous rate (SR) was computed during acquisition of the RA by averaging the discharge rate at 0 dB SPL across the entire frequency range. Dynamic range (DR) was manually derived from rate curves (see below) at CF; it is an estimate of dB range from spontaneous rate to firing rate saturation and is provided in 5 dB increments.

Threshold, Q10s and tuning curves: threshold (TH) levels reported were determined from the RA after each rate curve was three-point smoothed. The threshold was determined at each frequency as the SPL at which the rate equaled SR + 30 sp/s (i.e. essentially the same criteria used by adaptive tracking algorithms, e.g. Kiang and Moxon, 1974). The resulting three values on each side of the characteristic frequency were fit with a first order regression line. The resulting lines were used to determine the bandwidth at 10 dB above threshold. The tuning characteristic is reported as a Q10 value, where Q10 is equal to CF divided by bandwidth at 10 dB above threshold.

Peristimulus time and interspike interval histograms: PSTHs were generated at CF as described above, and were computed using a 60 msec analysis window with a 200μs binwidth. ISIHs were computed using a 50 msec analysis window with a 100μs binwidth.

Latency and rate curves: latency (Lat) values were derived from response area data. A program determined the three shortest first spike latencies observed at the three highest SPL values presented at CF and at one frequency step above and below CF. Stimuli were 50 ms long with a 3 ms cosine rise/fall with 5 repetitions (response areas were repeated using 10 repetitions if the unit was stable). Here, latency is the mean of the three shortest first spike latencies in ms, and these minimum latency values are included in figures showing distributions. Latency was

used to insure that the recordings were from CN neurons and not ANFs. The units classified as PLs here had latencies longer than those of PLn units, indicating these PLs were indeed 2nd order neurons and not ANFs.

Acoustic delay of the stimulus system was less than 300 μs and no compensation was made in calculating latencies. Rate curves at CF and wide-band noise RCs are included in figures if obtained.

Synchronization coefficient and coefficient of variation: two synchronization coefficients (SC) or so called vector strengths (Goldberg and Brown, 1969) were calculated in order to gain some appreciation for how well CN cell types in the monkey can phase lock within the RA and to amplitude modulation. RA-SC is the maximum SC value observed from the PSTH derived at CF, and that SC was determined only for cells whose CF was ≤ 2 kHz. MTF-SC is the maximum SC value observed at the AM modulation frequencies used for the MTF. The coefficient of variation (CV) is defined as the standard deviation/mean of the ISIH, and is reported for various parameters.

A total of 373 units were recorded of which 296 units could be assigned a response type. 159 response-defined units were recorded in squirrel monkeys, 48 in macaques, and 89 in one marmoset. Descriptive statistics on response properties for a particular response type are only reported here if at least 5 units of that type were recorded from one species. However, values for each response property were typically taken from a subpopulation within the response type, since all response parameters were rarely obtained from an individual neuron. If the response parameter value was taken from a significantly smaller number of cells categorized within a single response type (e.g. MTF-SCs were recorded from 7 PL units out of a total of 44 PL neurons isolated in the squirrel monkey), then the number of units used to derive that response parameter is indicated. Standard deviations are shown only if response parameters from 5 neurons were determined.

Unit identification and figures: Species are identified as squirrel monkey (SM), cynomolgus macaque (CM), and marmoset (MM). In figures, units are identified by three descriptors: animal type, animal number, and unit number. For example, SM02-13 would indicate squirrel monkey 2, unit 13.

2.4. Response categories

Chopper units—The term “chopper” refers to units whose PSTHs exhibit peaks early in responses to short tone bursts at CF, and the period of those peaks is not related to the period of the tone stimulus except for low stimulus frequencies. The coefficient of variation (CV) computed from the interspike interval histogram provides a measure of the regularity of the firing pattern, with lower CVs indicating a more regular discharge. While the distribution of CV values does not have distinct modes, we have divided choppers into “sustained choppers” (Cs) and “transient choppers” (Ct) on the basis of whether the CV is less than or greater than 0.3 (Rhode and Smith, 1986a,b). Young et al., (1988) used a CV of 0.35 to distinguish regular and irregular choppers. Both Cs and Ct units have been shown to arise from multipolar cells (Smith and Rhode, 1989).

A separate population of wide-band choppers (Cw units) is observed in the DCN of cats and gerbils. These units fire slowly but regularly, resulting in widely spaced modes in the PSTH, in a low CV value, and in a regular chopper classification. This response type might be associated with fusiform cells (Rhode et al., 1983a; Smith and Rhode, 1985; Rhode and Smith, 1986b; Hancock and Voigt, 2002).

Another method for distinguishing chopper types employs an analysis of the degree of regularity in the discharge pattern over the duration of the stimulus (Bourk, 1976; Young et al. 1988). Using a regularity analysis that includes the evolution of discharge rate and the CV as a function of stimulus time, another chopper pattern can be described. Young et al. (1988) noted that Ct's mean discharge rate decreased and CV increased with stimulus time, and in contrast, Cs units had little rate adaptation and a constant CV. They termed Ct's irregular and Cs's regular choppers. Young et al. (1988) further noted that some irregular choppers, termed Cu choppers, exhibit a decreased CV and may or may not show rate adaptation with stimulus time. Here we classify choppers as Ct, Cs, and Cw units, primarily depending on their PSTH and ISIH patterns and the 0.3 CV criterion as derived from the ISIH (e.g. units labeled Ct have significant rate adaptation and usually have a skewed ISIH distribution or 3rd central moment). We continue to use the simpler classification method for the population statistics in this paper.

Primary-like units—Primarily-like units have PSTHs and ISIHs that are similar to auditory nerve fiber responses. These response patterns arise from bushy cells in the VCN. They are usually separated into PL and PLn subcategories, and PLn units display a characteristic 0.5 – 2.0 ms notch in the PSTH immediately after the onset response. PL units arise from spherical bushy cells and the PLn units from globular/bushy cells in the nerve root area of the VCN (Smith and Rhode, 1987; Smith et al., 1993). PL and PLn classifications are used in this paper (Pfeiffer, 1966; Bourk, 1976; Blackburn and Sachs, 1989).

Onset units—Several onset unit categories with distinct PSTHs begin with a prominent initial discharge peak that reflects a well-timed spike for every tone pip. Because of this strong onset response, the ratio of the discharge rate at this peak is high relative to the steady-state discharge rate for these unit types. Onset-ideal or onset-initial (OnI) units generate a single spike at the beginning of the tone pip, and can discharge at a precise phase to every cycle of a low frequency tone (< 500 – 800 Hz). These response types are associated with octopus cells (Godfrey et al., 1975a). Onset-choppers (OnC) exhibit an onset response plus a chopping pattern later in the PSTH; these response types are associated with multipolar cells in cat that are found primarily in the PVCN (Smith and Rhode, 1989). Onset units with later activity (OnL) have a strong onset component and sustained activity further out in the PSTH, which can reach steady-state rates of up to 100 sp/s at high stimulus intensities (Godfrey et al., 1975a).

PLn units have a high peak-to-steady-state firing rate ratio, similar to onset units. For this reason, we pool OnI, OnC, OnL, and PLn units into the general "onset" category in this paper.

2.5. Dorsal cochlear nucleus response categories

Reconstructions of penetrations indicate that some activity was recorded from the DCN in the present experiments. Responses in the DCN have been classified on the basis of PSTH patterns as: pauser (P), buildup (B), pauser/chopper (P/C), pauser/buildup/chopper (PBC), and chopper wideband (Cw) (Godfrey et al., 1975b; Rhode et al., 1983b). Evans and Nelson (1973) used a type I through type V designation for DCN neurons: type I (TI) have AN response maps; type II (T2) cells have no spontaneous activity, non-monotonic rate curves and are inhibited by noise; type four (TIV) cells have a low threshold excitatory region at CF with inhibitory sidebands; and type five (TV) units are inhibited over their entire response area. Because we isolated 10 P and 17 Cw units but less than 2 each of other DCN unit types, we have combined all B, P/C, PBC, T2, TIV, and TV neurons into another "all others" category.

3. Results

3.1. Response Areas, Response Properties, and Histograms

Figure 1 to Figure 3 show representative response areas, PSTHs, rate and first spike latency curves, and ISIHs for units from all three monkey species of the 8 response types commonly used to describe CN neurons. The CV *vs* time is plotted with each PSTH, and indicated for each ISIH distribution. Noise RCs are included if obtained (col. 3). Figure 1 illustrates the response measures for three chopper units, a chopper with widely spaced PSTH modes (Cw) and a Cs unit from the squirrel monkey, and a Ct unit from the marmoset.

SM04-4 (top row, Fig.1) was a Cw unit with a CF of 3.9 kHz, SR of 1 spike/s, TH of 29 dB, and Q10 of 1.9. This chopper-wideband classification is based on the large mean interspike interval of nearly 11 ms between the modes in the PSTH. The unit displayed monotonic pure tone and noise RCs, and had a DR of 65 dB and latency at CF of 4.4 ms. SM04-4 did not phase lock well to low-frequency tones, and the maximum SC observed throughout the RA was 0.41. No MTF was established for this unit. Based on the penetration reconstruction, it is likely that SM04-4 was located in the DCN. Over an approximately 1 mm path, the electrode isolated units whose CFs progressively declined from about 7.5 kHz to below 1 kHz. The response type sequence of the isolated units was PL, buildup (B), Cw, pauser-buildup-chopper (PBC), and two OnCs.

SM01-12 (2^{nd} row, Fig, 1) was a Cs unit with a CV < 0.3, a CF of 3.3 kHz, SR of 2 spikes/second, TH of 30 dB, and Q10 of 3.2. The unit displayed a monotonic rate curve with a DR of 35 dB and latency at CF of 5.8 ms. The magnitude of phase locking was insignificant throughout its RA. No MTF was obtained for SM01-12. Based on the penetration reconstruction, it is likely that SM01-12 was located in the PVCN. Over a short electrode path of less than 500u below the CN surface, a Cw, 2 PLns, and a Cs unit were isolated in sequence. CFs for these units ranged from 2.4 – 4 kHz.

MM01-109 (3^{rd} row, Fig. 1) was characterized as a Ct unit and had a CF of 5.3 kHz, SR of 15 spikes/second, TH of 28 dB, and Q10 of 6.6. The unit displayed a monotonic rate curve with a DR of 50 dB and 6.3 ms latency at CF. The unit phase locked well at lower frequencies with the maximum SC of 0.89 throughout the RA. A MTF was also obtained for this unit that showed decreasing SC values at higher SPL levels of AM modulation. Maximum MTF-SC values for this unit were 0.7 at 30 dB, 0.5 at 50 dB, and 0.3 at 60 dB, and it had a cutoff frequency of 200 Hz. The shape of MM01-109's MTF was lowpass. Based on the penetration reconstruction, MM01-109 was likely located in the AVCN. Over an electrode excursion of approximately 1800μm, 2 PL units were encountered, and then 6 Ct units. During this recording sequence, CFs progressively declined from 14.5 to 3.5 kHz.

Figure 2 documents OnC, OnI, and PLn units from the squirrel monkey; these units are shown together because onset activity is the predominant feature in each response category. The top row of Figure 2 illustrates responses from SM02-32, an OnC unit. SM02-32 had a CF of 1 kHz, SR of 7 spikes/second, TH of 23 dB, and Q10 of 1.6. The unit had monotonic tone and noise RCs and had a DR of about 70 dB and a latency of 5.0 ms. The response map shows broad tuning, as indicated by the low Q10 of 1.6 that is typical of OnC units. The SC was 0.18 at CF, while the maximum SC obtained over the entire RA was 0.84. No MTF was obtained from this unit. Based on the penetration reconstruction, it is likely that SM02-32 was located in the PVCN. Over an electrode excursion of approximately 1500 μm, 1 Ct unit, an On unit, the OnC unit, 2 Ct units, and 3 PL units were encountered. During this recording sequence, CFs were 7 kHz and 4.6 kHz for the Ct and On units, and then dropped to below 1.7 kHz for the remaining units isolated.

The second row in Figure 2 shows SM01-8, a PLn unit. SM01-8 had a CF of 2.5 kHz, SR of 74 spikes/second, TH of 21 dB, and Q10 of 3.8. The unit displayed monotonic tone and noise RCs, approximately a 30 dB DR and a latency of 2.7 ms. The SC was 0.05 at CF, and the maximum SC of the MTF was 0.36. The shape of SM01-8's MTF was bandpass. Unit SM01-8 was located approximately 1500 μm below the brain surface, and since no other units were isolated in this penetration, we cannot determine its location within the CN complex.

The third row of Figure 2 shows SM09-7, an OnI unit. SM09-7 had a CF of 10 kHz, SR of 3 spikes/second, TH of 25 dB, and Q10 of 4.2. The unit had monotonic tone and noise RCs and a DR of about 30 dB. The latency for SM09-7 was 3.0 ms, and it was broadly tuned. The PST SC was insignificant at CF, but the highest SC within the RA was 0.83. Based on a dorsal-to-ventral penetration reconstruction plotting unit electrode depth *vs* CF, we believe SM09-7 might have been located in the PVCN. Over an electrode excursion of less than 800μm, 3 Ct units, 1 OnI unit, and 2 units that could not be classified were encountered. CFs for the 6 units isolated were in the 7.8 to 23 kHz range, with no consistent tonotopic pattern.

Figure 3 shows data from PL units isolated in each species, and includes PL neurons with low, middle, and higher CFs. The top row illustrates CM04-15, a PL unit with a CF of 1.1 kHz, SR < 1 spike/second, TH of 52 dB, and Q10 of 2.4. The unit displayed a monotonic rate curve with a dynamic range of about 35 dB, and had a latency of 5.5 ms. As is clear from the ISIH, the unit tightly encoded the stimulus waveform at lower frequencies. The maximum SC at CF was 0.79, and the maximum SC throughout RA was 0.9. No MTF was obtained from this unit. Based on the penetration reconstruction, it is likely CM04-15 was located in the AVCN. After traveling about 1 mm, the electrode isolated four neurons over approximately 450 um, including 3 PL and 1 OnC units. The PL units had CFs between 1.0 and 1.6 kHz, and the OnC's CF was 3.4 kHz.

The second row documents responses from SM09-28, a PL unit with a CF of 1.8 kHz, SR of 8 spikes/second, TH of 37 dB, and Q10 of 2.3. The rate curves at CF and using noise were monotonic, and the minimum latency at CF was 3.9 ms. The maximum SC at CF for this PL unit was 0.51, while the maximum SC at lower frequencies in the RA was 0.95 and its maximum MTF-SC was 0.59. The shape of the MTF was lowpass. The dorsal to ventral penetration reconstruction also indicates SM09-28 was likely located in AVCN. Here, 2 Ct units with CFs of 10.2 and 7.4 kHz were isolated about 700 um below the brain surface, and then 6 PL units were found over the next 700 um. CFs for the 2 most dorsal PL units were 8.0 kHz, and then dropped from 1.8 kHz for sm09-28 to around 600 Hz for the remaining 3 PL units.

The last row in Figure 3 shows MM01-15, a PL unit. MM01-15 had a CF of 6.8 kHz, SR of 42 spikes/second, TH of 17 dB, and Q10 of 5.4. The unit displayed a monotonic rate curve and had a DR of about 20 dB and a latency of 2.9 ms. MM01-15 did not phase lock well, and its MTF-SC was 0.06. Iso-intensity RA curves for MM01-15 also demonstrated inhibitory side bands on both sides of CF (see Methods).

Based on a dorsal-to-ventral reconstruction of the penetration plotting unit electrode depth *vs* CF, we believe MM01-15 might have been located in the AVCN. Over an electrode excursion of approximately 1600 μm, 12 neurons were isolated, including 7 PL, 3 PLN, 1 P, and 1 unclassified unit. During this recording sequence, the first 2 CFs (PLn and PL units) were around 6 kHz. The next 5 CFs (4 PL and 1 unclassified unit) jumped to 25 – 32 kHz, and the remaining CFs (2 PLn and 3 PL units) decreased from 6.8 to 0.9 kHz.

3.2. Chopper Responses

Figure 4 illustrates one marmoset unit (Fig. 4A) and three squirrel monkey units categorized as Cts (Figure 4B–D), and one squirrel monkey unit classified as a Cw (Figure 4E). Note that

the PSTH was shortened to 30 ms here for presentation purposes, but the response patterns illustrated in the first 30 ms continued throughout the tone burst stimuli. PSTHs from these units clearly demonstrate they were chopper units, and the ISIHs reflect distributions typically associated with Ct and Cw units. CV values were highest for the first three Ct units shown and lowest for the Cw unit, indicating a very regular discharge rate throughout the stimulus for the Cw neuron. The chopper in Figure 4C would be labeled Cu by the criteria of Young et al. (1988), i.e. a constant mean rate and decreasing CV as a function of time.

3.3. Distribution of Response Types

There were sufficient data for 296 units to determine response type. Table 1 summarizes the number of categorized units recorded for each species, and the percentage each response type represents for all monkeys combined. If data from the three monkey species are combined, Cw, Ct, and C_s units constitute approximately 36% of all units recorded, On, OnC, and OnI units about 10%, and PL and PLn units about 47%. DCN unit types (i.e. Cw, P, and "all other" units) accounted for about 12% of the neurons isolated. It is not possible to assess whether these recordings forma representative sample.

Based on the division of chopper response patterns by CV (i.e. CV values for Ct units are >0.3 and <0.3 for Cs units), there were fewer Cs than Ct units. As discussed in Methods, whether those units with a lower firing rate with CVs <0.3 should be classified as Cw or Ct units is problematic. Cw classification has been reserved for choppers found in the DCN with a maximum discharge rate less than 100 spikes/s. There were 84Ct, 5 Cs and 17 Cw units using a CV criterion of 0.3.

3.4. Descriptive Statistics for Response Types in Primate Species

If at least 5 neurons of a response type were recorded and a particular response parameter was obtained (typically on a subpopulation of the number of cells categorized within a response group), descriptive statistics for those cells in each monkey species are shown in Table 2–Table 5. These include mean and standard deviation (SD) values for SR, TH, DR, PST-SC, and MTF-SC. Note that because phase locking significantly decreases at higher frequencies (see e.g. Figure 6c below), these tables only include PST SC values derived from neurons with CFs ≤ 2 kHz.

3.4.1. Marmoset—Because the number of Ct and PL units studied in the marmoset is substantially higher than PLn neurons, it is most useful to compare their response values. These two populations did not show significant differences with regard to SR, TH, Q10s or DR. While only 2 Ct and 3 PL units had CFs ≤ 2 kHz, the PL units appeared to phase lock significantly better to short tone bursts at CFs. However, MTF-SCs were determined for 22 Ct and 22 PL units in the marmoset, and both those population types were able to phase lock well to the waveform envelop of AM stimuli.

3.4.2. Cynomolgus macaque—Most data from the Cynomolgus macaques were derived from a single animal, and thresholds increased during that experiment. PL units were the largest population studied (27), and OnC (6) and On (5) categories the next most populous. Average spontaneous rates were 38.7 sp/s for PL units, 44.9 sp/s for OnC's, and 16.1 sp/s for On units. Of the 27 PL neurons isolated, 12 had CFs ≤ 2 kHz. As in the marmoset, these low frequency PL units phase-locked well to short tone bursts at CF, and their mean PST SC at CF was 0.64. Only 1 MTF-SC value could be obtained; that value was 0.74, and it was obtained from a PL unit with a CF of 18 kHz. TH values are not included because of the changes observed during the best experiment.

3.4.3. Squirrel monkey—The squirrel monkey experiments yielded the largest amount of data. Here, PLn and Ct units had substantially higher SRs than Cw, On, and OnC response types, but TH values for these 6 response types did not appear to be significantly different. OnC units had the lowest Q10 values and the highest DR, but these values are based on a limited sample of 8 neurons.

Cw, Ct, PL, and PLn neurons were the largest populations isolated in the squirrel monkey. Here, 7 Ct, 23 PL, and 3 PLn units had CFs ≤ 2 kHz, and PST SCs for the PL response groups appeared to be much higher than the CT cells (single sided t-test $P < .005$). For each of these 6 response types shown in Table 4, MTF-SC values indicated these cell types could clearly encode the envelop of an AM stimulus. This MTF-SC parameter population included 3 Cw, 27 Ct, 2 OnC, 7 PL, and 4 PLn cells; a single On unit had a MTF maximum SC of 0.88.

3.5. Temporal Modulation Transfer Functions for Different Response Types

Figure 5 A–F show the temporal modulation transfer function synchronization coefficients as a function of AM modulation frequency for six example Ct, PL, and PLn units, and are taken from squirrel monkey and marmoset neurons. The MTFs for chopper units illustrate both lowpass (A) and bandpass (B) characteristics that either maintained (A,B) or changed (C) that form over the 40 dB intensity range. Most choppers had a lowpass MTF shape (41 of 59, 69%). Those classified as bandpass were usually lowpass at low intensities and became bandpass by 50 to 70 dB SPL. Bandpass center frequency was usually between 200 and 800 Hz, with 300 Hz occurring most often, although the Ct unit in Fig. 5B had a bandpass MTF at all intensities with a very low center frequency (~ 100 Hz). Cutoff frequencies of the MTFs were estimated as the frequency where the magnitude of the MTF dropped below 0.2, and these ranged from 200 to 1000 Hz, with the majority below 500 Hz.

Primarylike units more often had MTFs that were lowpass (Fig. 5D). The exceptions were PLn units that often had bandpass MTFs (Fig. 5E). Some PL units had a bandpass MTF at high levels (Fig. 5F).

The maximum MTF-SCs exceeded 0.5, which is the value that would be expected if the modulating waveform were reproduced by the instantaneous firing pattern. Another point to note is that as intensity is increased the magnitude of the MTF remains high, thereby preserving the temporal code. While the magnitude of the MTF typically decreased with increasing intensity for both choppers and primarylike units, the decrease was small for the Ct unit in Fig. 5B and the PLn unit in Fig. 5E. In other words, a robust temporal code is preserved in some units. In contrast, the rate-MTFs (not shown) were nearly uniformly flat and increased with intensity for choppers and primarylike units. Therefore, there is no AM coding in the average discharge rate of these unit types.

3.6 Distribution of Response Properties for Selected Response Types

Table 1 summarizes the total population of neurons encountered during these experiments, and Figure 6–Figure 9 show the actual distribution of Q10, latency, PST-SC, MTF-SC, threshold, and spontaneous rate values for the seven largest subpopulations of response types from this table. These include: Cw units from the squirrel monkey, Ct units from the marmoset and squirrel monkey, PL units from all three subspecies, and PLn units from the squirrel monkey. Since some of these response properties were not obtained for all units, Figure 6–Figure 9 only illustrate data if at least 4 values were derived for each property.

Figure 6A–F shows the distributions of Q10, latency, PST-SC, MTF-SC, threshold, and spontaneous rate values for CT units recorded in the marmoset and squirrel monkey. The MTF-SC value is the maximum SC value observed over the range of AM modulation frequencies,

which was usually varied from 50 or 100 – 2550 Hz in 100 Hz steps. Regression lines have been fitted to the latency data from both species in Figure 6B, with outliers exceeding 8 ms excluded (i.e. 1 point in the squirrel monkey and 3 in the marmoset). The shape of the resulting curves are similar to those observed in other animals. Ct cell latencies decrease approximately 2 ms as CFs are increased from 500 Hz to 30 kHz. Threshold distributions (Fig. 6E) are similar for both species while squirrel monkey cell spontaneous rates are somewhat lower than those of marmoset CT cells (Fig. 6F).

Figure 7 A–D displays the distribution of Q10, latency, threshold, and spontaneous rate for Cw units in the squirrel monkey. Only 2 units could be assigned PST SC values and 3 units MTF values, so those data are not included here.

Figure 8 A–D show the distribution of Q10, latency, PST-SC, MTF-SC, threshold, and spontaneous rate values for PL units recorded in the squirrel monkey, marmoset, and cynomolgus macaque. The latency values in Figure 8B were obtained from rate curves derived from the RA at CF, and a regression line has been fitted to the combined data from the three species. Here, latencies for PL units with characteristic frequencies down to 500 Hz are approximately 4.5 ms, and decrease to approximately 2.5 ms for PLs with characteristic frequencies greater than 30 kHz. Squirrel monkey SCs (Fig. 8C) are somewhat lower than for the other species. SCs are nearly zero by 4 kHz in all species. The temporal modulation function SCs have an especially wide range from 0.25 to 0.95 in the region of 10 kHz CFs. Thresholds were higher in the macaques, and as explained in Methods, this might be due in part to calibration difficulties in this species. Spontaneous rates were higher in marmosets than squirrel monkey (single-sided t-test, $P < 0.05$ while the two-sided t-test yielded $P < 0.1$).

Figure 9 (A–F) shows the distribution of Q10, latency, PST SC, MTF-SC, threshold, and spontaneous rate values for PLN units recorded in the squirrel monkey and marmoset. The latency values in Figure 9B were obtained from rate curves derived from the RA at CF. A regression line has been fitted to the combined data from both species, but the two highest points just above a CF of 20 kHz were excluded from the fit. Here, latencies for PLn units are approximately 3.5 ms for neurons with characteristic frequencies near 500 Hz, and drop to approximately 2 ms for PLns with characteristic frequencies above 20 kHz. The average spontaneous rate (F) is nearly 50 spikes/s.

3.7. Summary Statistics for Three Primate Species

In Table 4, we have combined response parameter values derived from the 7 largest response categories in squirrel monkeys and marmosets (see Table 1), and each response type contained a minimum of 5 units. Response parameter values shown are SR, TH, PST SC for units with CFs <= 2 kHz, and MTF-SC. SD values were calculated only if at least 5 values were available for that particular response parameter.

When data are combined, three features from the data set appear to be the most salient:

1. units in the general onset category (i.e. On and OnC units) have a lower SR than found in the other major response groups.
2. For units with CFs <= 2 kHz, PL neurons phase lock much better than CT cells.
3. Cw, Ct, PL and PLn response types appear to encode the waveform envelop well, as measured by the MTF-SC value. It is also worth noting that although MTF-SC values were determined in a total of 9 other units in the On, OnC, and P categories, the lowest mean MTF-SC for those small populations was 0.74.

4. Discussion

These experiments provide the first glimpse of response properties of CN neurons in the monkey. Perhaps the most salient feature of these data is that CN neurons in three different primate species fall into the same classes of responses that have been observed in other mammals used for auditory studies. As in other mammalian species, the predominant response types in the VCN of these primates fall into three major groups: chopper, onset, and primary-like units. In the DCN the most commonly recorded temporal firing patterns were Cw responses.

4.1. Input to the cochlear nuclei through the VIIIth nerve

Decades ago, monkeys were used to study the response properties of VIIIth nerve fibers in several of the seminal works on the auditory system, but typically these studies analyzed the response properties of a few nerve fibers in depth without generating population data (Anderson, et al., 1971; Brugge, et al., 1969; Hind et al., 1967; Rose et al., 1967, 1969, 1971; Ruggero, 1973). Later, Liberman (1978) showed that in cats auditory nerve fibers fall into three distinct populations that differ in their spontaneous firing rates: low-SR (<0.5 spikes/s), mid-SR (0.5–18 spikes/s) and high-SR (>18 spikes/s). Fibers with differing spontaneous firing rates differ in their thresholds, dynamic range, maximal firing rates, their morphology and their targets (Liberman, 1978; Schalk and Sachs, 1980; Fekete et al., 1984; Rouiller et al., 1986; Winter et al., 1990; Liberman, 1991, 1993). The differences in spontaneous firing rates are not affected by anesthetic (Kim et al., 1990). It has been suggested that the differences associated with differences in spontaneous firing rates exist in all mammals (Schmiedt, 1989; Winter et al., 1990). The question whether auditory nerve fibers in primates are subdivided in these same ways has not been addressed.

Because this important issue has not been addressed directly in the literature, we have compiled published and unpublished population data on the spontaneous rate of VIIIth nerve fibers in monkeys (Figure 10, Table 5). Nomoto et al. (1964) showed a histogram of the spontaneous rate distribution for 78 VIIIth nerve fibers in 32 monkeys representing 4 different types of macaque, and Katsuki (1966) republished the same data. Geisler et al. (personal communication, 2008) have provided spontaneous rate data from 218 VIIIth nerve fibers recorded from squirrel monkeys (Geisler, et al., 1974). Geisler et al. data are shown in Figure 10A. It is comparable to the cat VIIIth nerve spontaneous rate distribution in Figure 10B (from Rhode and Smith, 1984, Rhode and Greenberg, 1997).

If these monkey and cat data are compared using the Liberman (1978) criteria of low- SR (< 0.5spikes/s), mid-SR (0.5–18 splikes/s), and high-SR (>18 splike/s), then in order, the percentage of units for Liberman, Geisler et al. and Rhode and Smith data is: low-SR: 16%: 11%:21%; mid-SR: 23%:46%:27%; and high-SR: 61%: 43%:52%. However, the Geisler et al. VIII nerve rates were read off of a hand plotted graph and subject to some inaccuracy. If one allows that the low-SR category to be 0–1 spike/s for the Geisler et al results, then the number of low-SR fibers in the squirrel monkey is 21%. It appears that the monkey distributions are reasonably similar to cat given the limitations of the data.

In addition, Rose et al. (1971) reported spontaneous rates from a sample of 124 VIIIth nerve fibers in the squirrel monkey and described the following distribution: 23% from 0 – 10 spikes/second, 37% from 11 – 50 spikes/second, and 40% from 51 – 110 spikes/second. Table 5 presents a summary of all spontaneous rate data we believe are currently available for primates.

The spontaneous firing rates in the auditory nerve of primates are nearly evenly distributed between 10 and 110 spikes/s, but there is a low-SR mode with a significant number of fibers. These data indicate that similar distinctions between auditory nerve fiber with low spontaneous

rates may exist in primates as in cats. Whether the distinctions between medium and high SR fibers are less clear or reduced by pooling is uncertain.

4.2. Frequency tuning properties

One of the fundamental properties of units in the auditory system is their tuning, which is most commonly measured by Q10. A recent controversy as to whether humans have more sharply tuned auditory nerve fibers than other well-studied species raises the question whether tuning is different in primates and non-primates. Shera et al. (2002) used behavioral measures and the properties of otoacoustic emissions to estimate Q10's in humans. They concluded that Q10's were grossly underestimated for humans. In contrast, Ruggero and Temchin (2005) reviewed the available literature on tuning and concluded that there was no convincing evidence that humans had exceptional tuning in their cochleas, and that human tuning was comparable to mammals and birds.

In this study, we present Q10 distributions for a variety of primate CN neurons that resemble those found in cats and rodents. These data indicate that tuning in primates resembles that of cats and rodents, supporting Ruggero and Temchin's conclusion. Joris et al. (2006) report that old world monkeys have somewhat higher Q10's, especially in the 10 kHz region, than rodents and cats and that macaque tuning curves have no 'tails'. We found that both marmoset and squirrel monkey tuning curves have tails. In a single macaque, the majority of tuning curves did not have tails but because thresholds were relatively high in this monkey, the presence of tuning curve tails could have been obscured.

4.3. Latency, Response Categories, and Cochlear Length

Anatomical studies have determined cochlear length in macaques and squirrel monkeys (Igarashi et al., 1968; Greenwood; 1990). The basilar membrane is about 23 mm long in the squirrel monkey and 23–26 mm in macaques, distances which are similar to the 25 mm reported by Liberman (1982) for the cat. Because basilar membrane lengths appear to be similar for the primates studied, we have combined latency data for PL and PLn cell classes in the different primates and fitted regression lines to those data. These regression lines indicate that PLn units have approximately 1 ms shorter latencies than Ct and PL units with like characteristic frequencies, and that Ct and PL units have similar latencies (Fig. 6B, Fig. 8B, & Fig. 9B). Marmoset Ct latencies are somewhat longer than those of squirrel monkey. However, only one marmoset was studied, and since other marmoset CN cell type latencies were similar in macaques and squirrel monkeys, a true population study would be required to confirm any difference. Nevertheless, these general results are consistent with our own observations in the cochlear nucleus of the cat (Rhode and Greenberg, 1994). Young and Sachs also report a difference in latency in cats but they find that chopper units have longer latencies than PL units (Young and Sachs, 2008). Presumably there is a discrepancy in the way units are identified. Overall, latencies in these three cell types appear to behave in primates as they do in other mammals.

4.4. Response Types, Cell Types and Population Distribution

The same anatomical cell types exist in primate and human CN as in other mammals that have more commonly been used to study the auditory system. In primates (Moore and Osen, 1979 a,b; Adams, 1986; Adams, 1997) as in other mammals (Lorente de Nó, 1981; Brawer et al., 1974; Osen, 1969; Cant, 1981; Tolbert and Morest, 1982), the major cell types in the ventral cochlear nucleus include bushy, multipolar and octopus cells. The similarity of physiological response properties used to analyze the organization and function of the CN in other mammals suggests that the same correlations hold between anatomical cell type and physiological response properties in primates and man (Evans and Nelson, 1973; Feng, et al., 1994; Ostapoff,

et al., 1994; Pfeiffer, 1966; Rhode et al., 1983a,[b]; Rhode and Smith, 1986a,[b]; Rhode and Greenberg, 1992; Young and Brownell, 1976; Young and Davis, 2002; Palmer et al., 2003).

Of the 17 response types that were isolated and recorded, 6 were commonly encountered in what was likely the VCN: Ct, On, OnC, P, PL, and PLn. The PLs and Cts were the most populous, constituting about 65% of the total units encountered. The chopper types documented in these studies suggest that there are strong similarities between primate chopper response types and those observed in other mammals commonly used in auditory studies. The present study encountered relatively fewer Cs and relatively more Ct units in primates than in cats, where the proportion of Cs and Ct units were nearly equal (Rhode et al., 1983a; Rhode and Smith, 1986a). The distribution of CV's for cat chopper units was lower than in primates. In primates the chopping appeared less regular and had broader ISIH's. Using a slightly different definition for Cs and Ct, CVs < or > 0.35, Young et al. (1988) reported 34 Cs, 6 Ct and 9 Cu choppers in cats. Our present results indicate that if one takes into account the presence or absence of rate adaptation and adaptation of the CV, then there are 5 Cs, 64 Ct and 19 Cu choppers combined for squirrel and marmoset monkeys (i.e. 19 Ct units are reclassified as Cu units). If we restrict the response categorization to CVs < or > 0.35, then there are nearly equal numbers of Cs and Ct units.

Some choppers in primates exhibit a decreasing CV with duration of the stimulus. Similar choppers were found in cat and were classified as Cu units by Young et al. (1988). Irregularity can arise from inhibition (Banks and Sachs, 1991); an early, short duration inhibition could account for the initial low regularity and also the later increased regularity. Inhibitory sidebands were commonly observed on the high frequency side of CF in monkey chopper units. Inhibitory sidebands have also been found in cat chopper units (Rhode and Greenberg, 1992; Paolini et al., 2005). Intracellular studies have identified other distinguishing features of choppers. There appear to be separate inhibitory inputs to choppers that either affect firing early in the tone response or later during the steady-state response (Paolini et al., 2005), and inhibitory sidebands are often present in a chopper's response area, although spontaneous activity is required to observe them.

Ct units observed in this study did not appear to have a particularly wide dynamic range. While choppers also have a limited dynamic range in other species studied to date, Lai et al. (1994) proposed that Ct units could provide a method of encoding speech sounds over a wide dynamic range by virtue of the placement of high-SR ANFs distally on the stellate dendrites, low-SR ANFs closer to the soma, and an inhibitory input between the two. This concept would enable low threshold ANFs to fire Cts at low stimulus levels and higher threshold ANFs with a somewhat larger dynamic range to drive the units at higher levels.

Cw units are not fully understood in cats or primates. In primates, approximately 6% of all categorized units had the low maximum firing rates and low CV that characterize Cw. Most of these units were recorded dorsally in the recording track, indicating that they were likely to have been recorded from the DCN. This category may, however, also include units in the VCN; Rhode and Smith (1986a) did not observe Cw units in the PVCN in cat but Godfrey et al. (1975a) did report finding some. In the present study, there was a propensity for choppers to be Ct units, and there were a significant number of choppers with a low maximum firing rate and low CV, as illustrated in the PSTHs and ISIHs of Figure 4, characteristics that were not found in other mammals (Rhode and Greenberg, 1994; Rhode and Smith, 1986a; Young et al., 1988; Palmer et al., 2003; Paolini et al., 2005). That is, these units appeared similar to Cw's but were located in the VCN.

Cells with Cs patterns, and probably also Ct units, are likely to have been recorded from multipolar, or stellate, cells. Anatomical studies in cats indicate the existence of two types of

stellate cells in the VCN that differ in their dendritic shapes and somatic innervations, (Cant, 1981; Rhode et al., 1983a; Smith and Rhode, 1989). Stellate cells with Cs response patterns have been shown to project to the ipsilateral DCN through collateral ramifications of a main axon that exits through the trapezoid body to the contralateral superior olivary complex and ventral nucleus of the lateral lemniscus (Smith and Rhode, 1989; Smith et al., 1993). Similar cells have been described in mice (Oertel et al., 1990).

A smaller population of units responded at the onset of tones and were identified as On or Oc. Both these groups of neurons are broadly tuned; the sharp timing of firing produces a large peak in the PSTH at the onset of responses to tones. Although there are striking similarities between them, these neurons are likely to represent two distinct groups of neurons.

Neurons with Oc temporal response patters have been shown to correspond to type II multipolar cells (Cant, 1981; Smith and Rhode, 1989). These neurons project to the ipsilateral DCN and through the intermediate acoustic stria to the contralateral cochlear nucleus (Oertel et al., 1990; Needham and Paolini, 2003; Arnott et al., 2004). These neurons are likely to be glycinergic and inhibitory (Wenthold, 1987; Ferragamo et al., 1998; Needham and Paolini, 2003).

Neurons with On response patterns could be octopus cells. Except in responses to low-frequency tones, where every cycle behaves like the onset of a tone, octopus cells fire only once at the onset (Godfrey et al., 1975; Rhode et al., 1983a; Oertel et al., 2000; Smith et al., 2005). Octopus cells project through the intermediate acoustic stria to the contralateral superior paraolivary nucleus and ventral nucleus of the lateral lemniscus (Smith et al., 1993; Adams, 1997; Schofield and Cant, 1997; Smith et al., 2005)

4.5. Encoding of Stimulus Envelope

Shannon et al. (1995) demonstrated that the envelope of speech sounds was an essential element for speech perception. They created stimuli in which a small number of noise bands with different center frequencies were modulated with the speech envelope in the same band. Listeners recognized the speech with as few as four frequency channels indicating that the low frequency envelope portion of the speech signal plays an important role in perception.

AM studies in the cat auditory nerve have shown that there is little significant temporal information remaining in individual ANFs around 70 dB SPL (Joris and Yin, 1992; Rhode and Greenberg, 1994). In contrast, nearly every category of unit in the CN equals or betters the temporal code for AM seen in the VIIIth nerve (Frisina et al., 1990; Rhode and Greenberg, 1994; Rhode, 1994).

The modulation transfer functions provide a window into the ability of CN neurons to encode envelope information. MTF-SC's reported here indicate that primate CN neurons can temporally encode the stimulus envelope up to at least 600 Hz, and that some neurons can do so to 1 kHz. The higher frequency portion of this temporal coding was more prominent in the response of PLn neurons. About half of the Ct's have bandpass-shaped MTFs with maximums in the 200 – 400 Hz range for intensities of 50 and 70 dB SPL, and more likely low pass shapes at 30 dB SPL.

A feature that stands out in primate CN neurons' ability to encode AM is that most unit types often had higher MTF-SCs than we expected based on observations on AM in the AN. PLn units were especially effective AM encoders as were some Ct units. However, often significant MTF-SC's were only obtained over a limited frequency and intensity range, and this occurrence appears to be more common in primates than in cat (Rhode and Greenberg, 1994).

Finally, it should be noted that the MTF-SC decreased with increasing intensity in all units studied. This response is to be expected based on the behavior of the MTF-SC in the auditory nerve as a function of increasing intensity. In the cochlear nucleus, the convergence of auditory nerve fibers with different CFs and spontaneous rates likely ensures that there is a preservation of temporal information in those fibers that are not in a rate saturated state, even when others are in a saturated state and therefore can fire on any cycle of the carrier.

4.6. DCN unit response properties and distributions

The DCN of primates has a somewhat different morphology than that of non-primate mammals. In primates the number of granule cells seems to be reduced so that the molecular layer is less distinct than in other mammals (Moore, 1979a, b, 1980). More recently it has however been demonstrated that as in non-primates, granule cells within the DCN have unmyelinated axons that contact dendritic spines (Rubio et al., 2008). These findings suggest that the primate DCN may fundamentally be similarly organized.

In evaluating responses from the DCN, several factors need to be considered. It has long been appreciated that responses in the DCN are strongly affected by anesthetic (Evans and Nelson, 1972; Young and Brownell, 1976). Even in the absence of anesthetic, inputs to granule cells and thus granule cells themselves are likely to be unnaturally quiet. Granule cells receive strong input from somatosensory and vestibular input that is unlikely to be active when the heads of animals are immobilized to make recordings possible (Weinberg and Rustioni, 1987; Kanold and Young, 2001).

In the present experiments, Cw units were encountered more frequently than in cat (Rhode et al., 1983b). It is likely that many of the Cw units were recorded from the DCN but because the VCN was the primary focus of our study, this is a tentative conclusion. In contrast with the VCN, temporal firing patterns of units in the DCN are less consistent. In cats and gerbils, responses associated with fusiform cells can have a peak at the onset, generating a pauser (P) type histogram, but can also lack the onset peak to have a buildup (B) type response (Rhode et al., 1983b). When the firing rate is consistent and low, modes appear in the histogram and the PSTHs appear as Cw (Hancock and Voigt, 2002). The absence of response types that are often associated with the DCN (i.e. P, P/B, and B) could also arise from sampling biases. In primates, the DCN is displaced somewhat medially and overlaps only a minor aspect of the VCN, the portion of the CN which was the primary focus of this study.

Acknowledgments

We are greatly indebted to our colleagues, Donata Oertel, Don Sinex, and Phil Smith, for their review of this manuscript. This study was funded by NIDCD grant 17590.

References

Adams JC. Neuronal morphology in the human cochlear nucleus. Arch. Otolaryngol. Head Neck Surg 1986;112:1253–1261. [PubMed: 3533119]

Adams JC. Projections from octopus cells of the posteroventral cochlear nucleus to the ventral nucleus of the lateral lemniscus in cat and human. Auditory Neurosci 1997;3:335–350.

Anderson DJ, Rose JE, Hind JE, Brugge JF. Temporal position of discharges in single auditory nerve fibers within the cycle of a sine-wave stimulus: frequency and intensity effects. J. Acoust. Soc. Amer 1971;49:1131–1139. [PubMed: 4994692]

Arnott RH, Wallace MN, Shackleton TM, Palmer AR. Onset neurons in the anteroventral cochlear nucleus project to the dorsal cochlear nucleus. J. Assoc. Res. Otolaryngol 2004;5:1153–1170.

Banks MI, Sachs MB. Regularity analysis in a compartmental model of chopper units in the anteroventral cochlear nucleus. J. Neurophys 1991;65:606–629.

Blackburn CC, Sachs MB. Classification of unit response types in the anteroventral cochlear nuclei: PST histograms and regularity analysis. J. Neurophys 1989;62:1303–1329.

Bourk, TR. Electrical Responses of neural Units in the Anteroventral Cochlear Nucleus of the cat. (PhD thesis). Cambridge, MA: MIT Press; 1976.

Brawer JR, Morest DK, Kane EC. The neuronal architecture of the cochlear nucleus of the cat. J. Comp. Neurol 1974;155:251–300. [PubMed: 4134212]

Brugge JF, Anderson DJ, Hind JE, Rose JE. Time structure of discharges in single auditory nerve fibers of the squirrel monkey in response to complex periodic sounds. J. Neurophys 1969;32:386–401.

Cant NB. The fine structure of two types of stellate cells in the anterior division of the anteroventral cochlear nucleus of the cat. Neurosci 1981;6:243–265.

Dublin, W. Fundamentals of sensorineuronal auditory pathology. Springfield, IL: Charles C. Thomas; 1976.

Evans EF, Nelson PG. The response of single neurons in the cochlear nucleus of cat as a function of their location and anesthetic state. Exp. Brain res 1973;117:402–427. [PubMed: 4725899]

Fekete DM, Rouiller EM, Liberman MC, Ryugo DK. The central projections of intracellularly labeled auditory nerve fibers in cats. J. Comp. Neurol 1984;229:432–450. [PubMed: 6209306]

Feng JJ, Kuwada S, Ostapoff EM, Batra R, Morest DK. A physiological and structural study of neuron types in the cochlear nucleus. I. Intracellular responses to acoustic stimulation and current injection. J. Comp. Neurol 1994;346(1):1–18. [PubMed: 7962705]

Ferragamo MJ, Golding NL, Oertel D. Synaptic inputs to stellate cells in the ventral cochlear nucleus. J. Neurophys 1998;79:51–63.

Frisina RD, Smith RL, Chamberlain SC. Encoding amplitude modulation in the gerbil cochlear nucleus: I. A hierarchy of enhancement. Hear. Res 1990;44:99–122. [PubMed: 2329098]

Fuse G. Das ganglion ventrale und das tuberculum acusticum bei einigen säugern und beim menschen. Arb. Hirnanat. Inst., Zürich 1913;7:1–210.

Geisler CD, Rhode WS, Kennedy DT. Responses to tonal stimuli of single auditory nerve fibers and their relationship to basilar membrane motion in the squirrel monkey. J. Neurophys 1974;37:1156–1172.

Geisler CD, Rhode WS, Kennedy DT. Personal communication. 2008

Goldberg JM, Brown PB. Response of binaural neurons of dog superior olivary complex to dichotic tone stimuli: some physiological mechanisms of sound localization. J. Neurophys 1969;22:613–636.

Godfrey DA, Kiang NYS, Norris BE. Single unit activity in the posteroventral cochlear nucleus of the cat. J. Comp. Neurol 1975a;162:247–268. [PubMed: 1150921]

Godfrey DA, Kiang NYS, Norris BE. Single unit activity in the dorsal cochlear nucleus of the cat. J. Comp. Neurol 1975b;162:269–284. [PubMed: 1150922]

Greenwood DD. A cochlear frequency-position function for several species – 29 years later. J. Acoust. Soc. Amer 1990;87:2592–2605. [PubMed: 2373794]

Hancock KE, Voigt HF. Intracellularly labeled fusiform cells in the dorsal cochlear nucleus of the gerbil. I. Physiological response properties. J. Neurophys 2002;87:25005–25019.

Heiman-Patterson TD, Strominger NL. Morphological changes in the cochlear nuclear complex in primate phylogeny and development. J. Morphol 1985;186:289–306. [PubMed: 4087302]

Hind JE, Anderson DJ, Brugge JF, Rose JE. Coding of information pertaining to low-frequency tones in single auditory nerve fibers of the squirrel monkey. J. Neurophys 1967;30:794–816.

Igarashi M, Mahon RG, Konishi S. Comparative measurements of cochlear apparatus. J. Speech Hear. Res 1968;11:229–235. [PubMed: 4969678]

Joris PX, Carney LH, Smith PH, Yin TCT. Enhancement of neural synchronization in the anteroventral cochlear nucleus. I. Responses to tones at the characteristic frequency. J. Neurophys 1994a;71:1022–1036.

Joris PX, Ramirez CL, McLauglin M, van der Heijden M. Spectral and temporal properties of the auditory nerve in old-world monkeys. Assoc. Res. Otolaryn. Abst. 2006

Joris PX, Smith PH, Yin TCT. Enhancement of neural synchronization in the anteroventral cochlear nucleus. II. Responses in the tuning curve tail. J. Neurophys 1994b;71:1037–1051.

Joris PX, Yin TCT. Responses to amplitude-modulated tones in the auditory nerve of the cat. J. Acoust. Soc. Am 1992;91:215–232. [PubMed: 1737873]

Kanold PO, Young ED. Proprioceptive information from the pinna provides somatosensory input to cat dorsal cochlear nucleus. J. Neurosci 2001;21:7848–7858. [PubMed: 11567076]

Katsuki Y. Neural mechanism of hearing in cats and monkeys. Progress in Brain Res 1966;21:71–97.

Kiang NYS, Moxon EC. Tails of tuning curves of auditory-nerve fibers. J. Acoust. Soc. Am 1974;55:620–630. [PubMed: 4819862]

Kim DO, Chang SO, Sirianni JG. A population study of auditory-nerve fibers in unanesthetized decerebrate cats: response to pure tones. J. Acoust. Soc. Am 1990;87:1648–1655. [PubMed: 2341668]

Lai YC, Winslow RL, Sachs MB. A model of selective processing of auditory-nerve inputs by stellate cells of the antero-ventral cochlear nucleus. J. Comput. Neurosci 1994;1:167–194. [PubMed: 8792230]

Liberman MC. Auditory-nerve fiber responses from cats raised in a low-noise chamber. J. Acoust. Soc. Am 1978;63:442–455. [PubMed: 670542]

Liberman MC. The cochlear frequency map for the cat: Labeling auditory-nerve fibers of known characteristic frequency. J. Acoust. Soc. Am 1982;72:1441–1449. [PubMed: 7175031]

Liberman MC. Central projections of auditory-nerve fibers of differing spontaneous rate. I. Anteroventral cochlear nucleus. J. Comp. Neurol 1991;313:240–258. [PubMed: 1722487]

Liberman MC. Central projections of auditory nerve fibers of differing spontaneous rate, II: Posteroventral and dorsal cochlear nuclei. J. Comp. Neurol 1993;327:17–36. [PubMed: 8432906]

Lorente de Nó, R. The Primary Acoustic Nuclei. New York, NY: Raven Press; 1981.

Moore JK. The primary cochlear nuclei: loss of lamination as a phylogenetic process. J. Comp. Neurol 1980;193:609–629. [PubMed: 6777412]

Moore JK, Osen KK. The cochlear nuclei in man. Am. J. of Anat 1979a;154:393–418. [PubMed: 433789]

Moore JK, Osen KK. The human cochlear nuclei. Exp. Brain Res 1979b;II:36–44.

Moskowitz N. Comparative aspects of some features of the central auditory system of primates. Ann. N.Y. Acad. Sci 1969;167:357–369.

Needham K, Paolini AG. Fast inhibition underlies the transmission of auditory information between cochlear nuclei. J. Neurosci 2003;23:6357–6361. [PubMed: 12867521]

Nomoto M, Suga N, Katsuki Y. Discharge pattern and inhibition of primary auditory nerve fibers in the monkey. J. Neurophys 1964;27:768–787.

Oertel D, Bal R, Gardner SM, Smith PH, Joris PX. Detection of synchrony in the activity of auditory nerve fibers by octopus cells of the mammalian cochlear nucleus. Proc. Nat. Acad. Sci. USA 2000;97:11773–11779. [PubMed: 11050208]

Oertel, D.; Wu, SH.; Hirsch, JA. Electrical characteristics of cells and neuronal circuitry in the cochlear nuclei studied with intracellular recordings from brain slices. In: Edelman, GM.; Gall, WE.; Cowan, WM., editors. Auditory Function. New York: John Wiley and Sons; 1988. p. 313-336.

Oertel D, Wu SH, Garb MW, Dizack C. Mophology and physiology of cells in slice preparations of the posteroventral cochlear nucleus of mice. J. Comp. Neurol 1990;295:136–154. [PubMed: 2341631]

Olson, RE.; Yee, D.; Rhode, WS. Digital System – Version II. Madison, WI: University of Wisconsin Medical Electronics Laboratory and Department of Neurophysiology; 1985.

Osen KK. The intrinsic organization of the cochlear nuclei in the cat. Acta otolaryngologica 1969;67:352–359.

Ostapoff EM, Feng JJ, Morest DK. A physiological and structural study of neuron types in the cochlear nucleus. II. Neuron types and their structural correlation with response properties. J. Comp. Neurol 1994;346(1):19–42. [PubMed: 7962710]

Palmer AR, Wallace MN, Arnott RH, Shackleton TM. Morphology of physiologically characterized ventral cochlear nucleus stellate cells. Exp. Brain Res 2003;153:418–426. [PubMed: 12955380]

Paolini AG, Clarey JC, Needham K, Clark GM. Balanced inhibition and excitation underlies spike firing regularity in ventral cochlear nucleus chopper neurons. Eur. J. of Neurosci 2005;21:1236–1248. [PubMed: 15813933]

Pfeiffer RR. Classification of response patterns of spike discharges for units in the cochlear nucleus: tone burst stimulation. Exp. Brain Res 1966;1:220–235. [PubMed: 5920550]

Rhode WS. Temporal coding of 200% amplitude modulated signals in the ventral cochlear nucleus of cat. Hear. Res 1994;77:43–68. [PubMed: 7928738]

Rhode, WS.; Greenberg, S. Physiology of the cochlear nuclei. In: Popper, AN.; Fay, RR., editors. The Mammalian Auditory Pathway: Neurophysiology. New York: Springer-Verlag; 1992. p. 94-152.

Rhode WS, Greenberg S. Encoding of amplitude modulation in the cochlear nucleus of the cat. J. Neurophys 1994;71 1979–1825.

Rhode, WS.; Greenberg, SR. Coding of noise -embedded spectro-temporal information in the cochlear nucleus. In: Ainsworth, WA.; Evans, EF., editors. Cochlear Nucleus: Structure and Function in Relation to Modeling. JAI Press Inc.; 1997. p. 169-191.

Rhode WS, Geisler CD, Kennedy DT. Auditory nerve fiber responses to wide-band noise and tone combinations. J. Neurophys 1978;41:692–704.

Rhode WS, Oertel DO, Smith PH. Physiological response properties of cells labeled intracellularly with horseradish peroxidase in cat ventral cochlear nucleus. J. Comp. Neurol 1983a;213:448–463. [PubMed: 6300200]

Rhode WS, Smith PH, Oertel DO. Physiological response properties of cells labeled intracellularly with horseradish peroxidase in cat dorsal cochlear nucleus. J. Comp. Neurol 1983b;213:426–447. [PubMed: 6300199]

Rhode WS, Smith PH. Characteristics of tone-pip response patterns in relationship to spontaneous rate in cat auditory nerve fibers. Hear. Res 1985;28:259–268.

Rhode WS, Smith PH. Encoding timing and intensity in the ventral cochlear nucleus of the cat. J. Neurophys 1986a;56:261–286.

Rhode WS, Smith PH. Physiological studies on neurons in the dorsal cochlear nucleus of cat. J. Neurophys 1986b;56:287–307.

Rose JE, Brugge JF, Anderson DJ, Hind JE, Hind. Phase-locked response to low-frequency tones in single auditory nerve fibers of the squirrel monkey. J. Neurophys 1967;30:769–793.

Rose JE, Brugge JF, Anderson DJ, Hind JE, Hind. Some possible neural correlates of combination tones. J. Neurophys 1969;32:402–423.

Rose JE, Hind JE, Anderson DJ, Brugge JF. Some effects of stimulus intensity on response of auditory nerve fibers in the squirrel monkey. J. Neurophys 1971;34:685–699.

Rouiller EM, Cronin-Schreiber R, Fekete DM, Ryugo DK. The central projections of intracellularly labeled auditory nerve fibers in cats: an analysis of terminal morphology. J. Comp. Neurol 1986;249:261–278. [PubMed: 3734159]

Roullier EM, Ryugo D. Intracellular marking of physiologically characterized cells in the ventral cochlear nucleus of the cat. J. Comp. Neurol 1984;225:167–186. [PubMed: 6327782]

Rubio ME, Gudsnuk KA, Smith Y, Ryugo DK. Revealing the molecular layer of the primate dorsal cochlear nucleus. Neuroscience 2008;154:99–113. [PubMed: 18222048]

Ruggero MA. Response to noise of auditory nerve fibers in the squirrel monkey. J. Neurophys 1973;36:569–587.

Ruggero MA, Temchin AN. Unexceptional sharpness of frequency tuning in the human cochlea. Proc. Nat. Acad. Sci 2005;102:18614–18619. [PubMed: 16344475]

Ryan AF, Miller JM, Pfingst BE, Martin GK. Effects of reaction time performance on single-unit activity in the central auditory pathway of the rhesus macaque. J. Neuroscience 1984;4:298–308.

Schalk TB, Sachs MB. Nonlinearities in auditory-nerve fiber responses to bandlimited noise. J. Acoust. Soc. Am 1980;67:903–913. [PubMed: 7358915]

Schmiedt RA. Spontaneous rates, thresholds and tuning of auditory-nerve fibers in the gerbil: comparisons to cat data. Hear. Res 1989;42:23–35. [PubMed: 2584157]

Schofield BR, Cant NB. Ventral nucleus of the lateral lemniscus in guinea pigs: cytoarchitecture and inputs from the cochlear nucleus. J.Comp. Neurol 1997;379:363–385. [PubMed: 9067830]

Shannon RV, Zeng F-G, Kamath V, Wygonski J, Ekelid M. Speech recognition with primarily temporal cues. Science 1995;270:303–304. [PubMed: 7569981]

Shera C, Guinan JJ Jr, Oxenham AJ. Revised estimates of human cochlear tuning from otoacoustic and behavioral measurements. Proc. Nat. Acad. Sci 2002;99:3318–3323. [PubMed: 11867706]

Smith, PH.; Joris, PX.; Banks, MI.; Yin, TCT. Responses of cochlear nucleus cells and projections of their axons. In: Merchan, MA.; Juiz, JM.; Godfrey, DA.; Mugnaini, E., editors. The Mammalian Cochlear Nuclei, Organization and Function. New York and London: Plenum Press; 1993. p. 349-360.

Smith PH, Joris PX, Yin TCT. Projections of physiologically characterized spherical bushy cell axons from the cochlear nucleus of the cat: evidence for delay lines to the medial superior olive. J. Comp. Neurol 1993;331:245–260. [PubMed: 8509501]

Smith PH, Massie A, Joris PX. Acoustic stria: anatomy of physiologically characterized cells and their axonal projection patterns. J. Comp. Neurol 2005;482:349–371. [PubMed: 15669051]

Smith PH, Rhode WS. Electron microscopic features of physiologically characterized, HRP-labeled fusiform cells in the cat dorsal cochlear nucleus. J. Comp. Neurol 1985;237:127–143. [PubMed: 4044890]

Smith PH, Rhode WS. Characterization of HRP-labeled globular bushy cells in the cat anteroventral cochlear nucleus. J. Comp. Neurol 1987;266:360–376. [PubMed: 3693616]

Smith PH, Rhode WS. Structural and functional properties distinguish two types of multipolar cells in the ventral cochlear nucleus. J. Comp. Neurol 1989;282:595–616. [PubMed: 2723154]

Tolbert LP, Morest DK. The neuronal architecture of the anteroventral cochlear nucleus of the cat in the region of the nerve root: Golgi and Nissl methods. Neurosci 1982;7:3013–3030.

Weinberg RJ, Rustioni A. A cuneocochlear pathway in the rat. Neurosci 1987;20:209–219.

Wenthold RJ. Evidence for a glycinergic pathway connecting the two cochlear nuclei: an immunocytochemical and retrograde transport study. Brain Res 1987;415:183–187. [PubMed: 3304530]

Winter IM, Robertson D, Yates GK. Diversity of characteristic frequency rate-intensity functions in guinea pig auditory nerve fibres. Hear. Res 1990;45:191–202. [PubMed: 2358413]

Young ED, Brownell WE. Responses to tones and noise of single cells in dorsal cochlear nucleus of unanesthetized cats. J. Neurophys 1976;39:282–300.

Young, ED.; Davis, KA. Circuitry and function of the dorsal cochlear nucleus. In: Oertel, D.; Fay, RR.; Popper, AN., editors. Integrative Functions of the Mammalian Auditory Pathway. New York: Springer; 2002. p. 160-206.

Young, ED.; Oertel, D. Cochlear nucleus. In: Shepard, GM., editor. The synaptic organization of the brain. New York: Oxford University Press; 2004. p. 125-163.

Young ED, Robert JM, Shofner WP. Regularity and latency of units in the ventral cochlear nucleus: implications for unit classification and generation of response properties. J. Neurophys 1988;60:1–29.

Young ED, Sachs MB. Auditory nerve inputs to cochlear nucleus neurons studied with cross-correlation. Neurosci 2008;154:127–138.

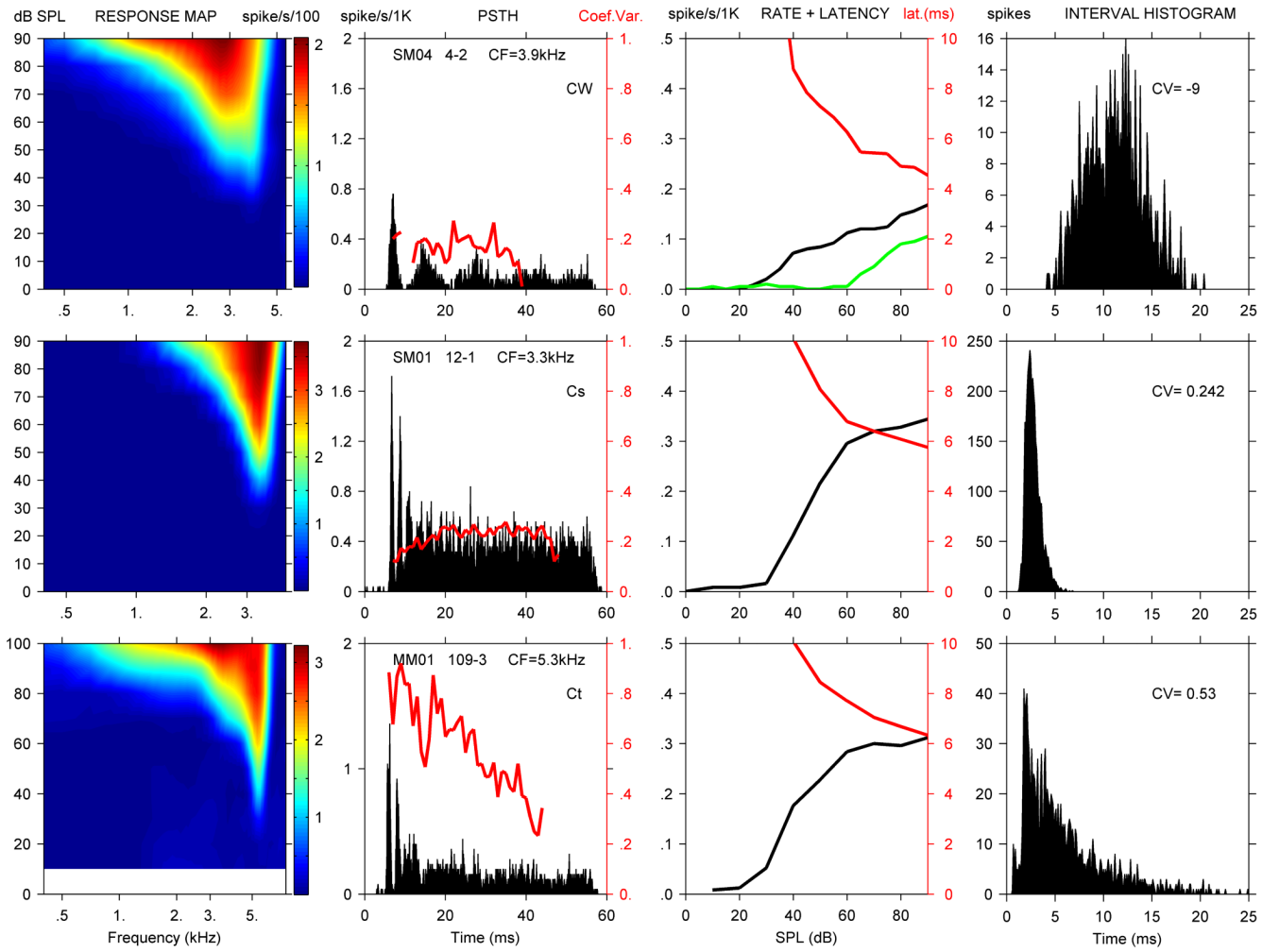

Figure 1.

RA (1st col.), PSTH with unit ID (2nd col.) and CV (red line), CF rate (black line) with noise rate curve (green line) and latency (red line) curves (3rd col.), and ISIH with CV value (4th col.) for 3 CN units. From the top down, squirrel monkey unit SM04-4 was classified as a Cw unit, squirrel monkey unit SM01-12 as a Cs unit and marmoset unit MM01-109 as a Ct unit based on their CVs (red lines in the 2nd col.). No data were taken below 10 dB for MM01-109, so that area of the response map is blanked. Note that the left ordinate in column 3 has units of spikes/s/1000, i.e. the maximum rate is 500 spikes/s, and also applies to Fig. 2 and Fig. 3.

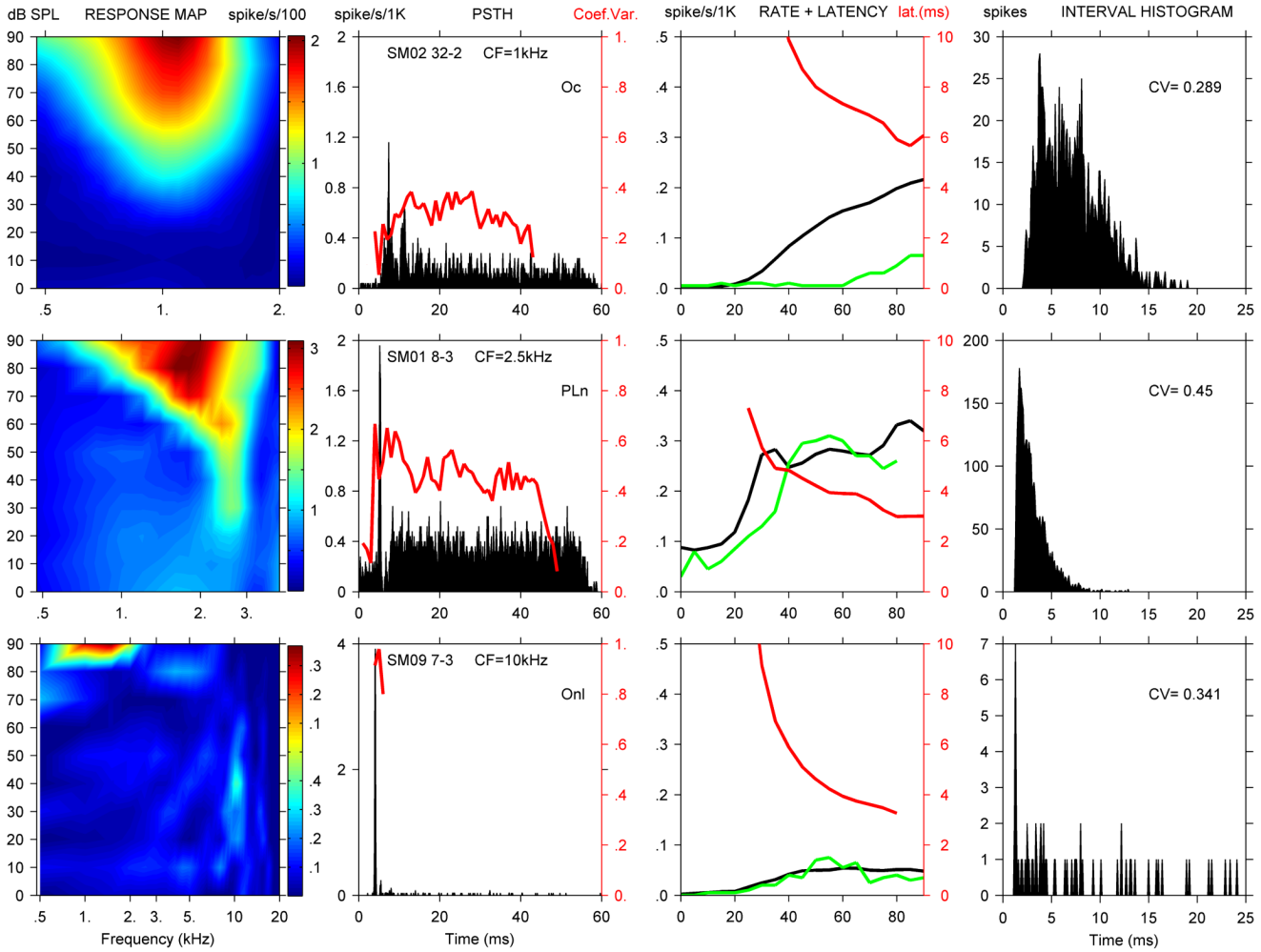

Figure 2.

RA (col. 1), PSTH with CV (col. 2), rate, noise rate, and latency curves (col. 3), and ISIH with CV value (col. 4) for 3 CN units with a prominent initial peak in their PSTH. From the top down, squirrel monkey unit SM02-32 was classified as an OnC unit, squirrel monkey unit SM01-8 as a PLn unit, and squirrel monkey unit SM09-7 as an OnI unit. Line colors as in Figure 1.

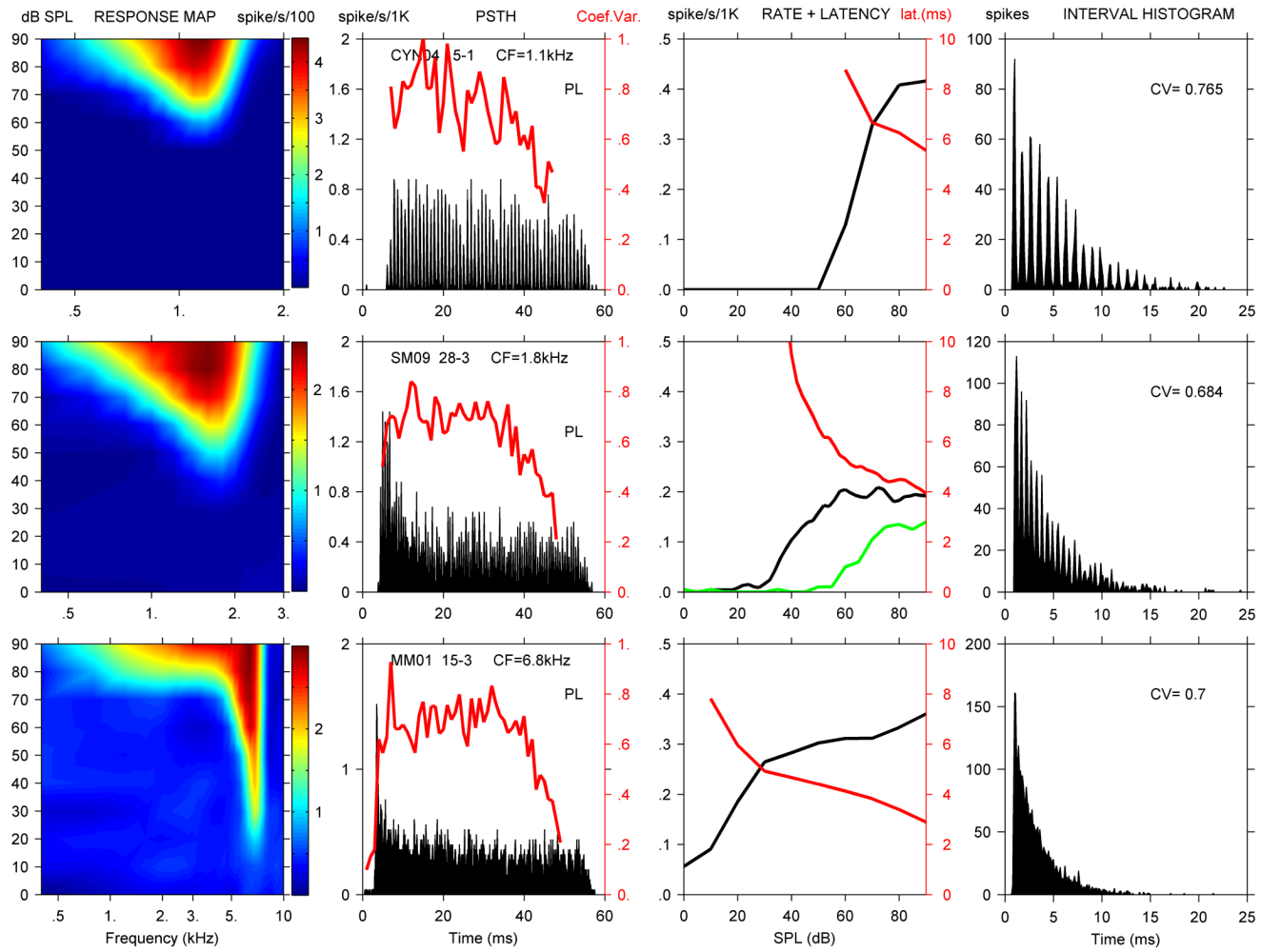

Figure 3.

RA (col. 1), PSTH with CV (col. 2), rate, noise rate, and latency curves (col. 3), and ISIH with CV value (col. 4) for PL units isolated in each species. From the top down, cynomolgus unit CM04-15 had a CF of 1.1 kHz, squirrel monkey unit SM09-28 had a CF of 1.8 kHz, and marmoset unit MM01-15 had a CF of 6.8 kHz. Line colors as in Figure 1.

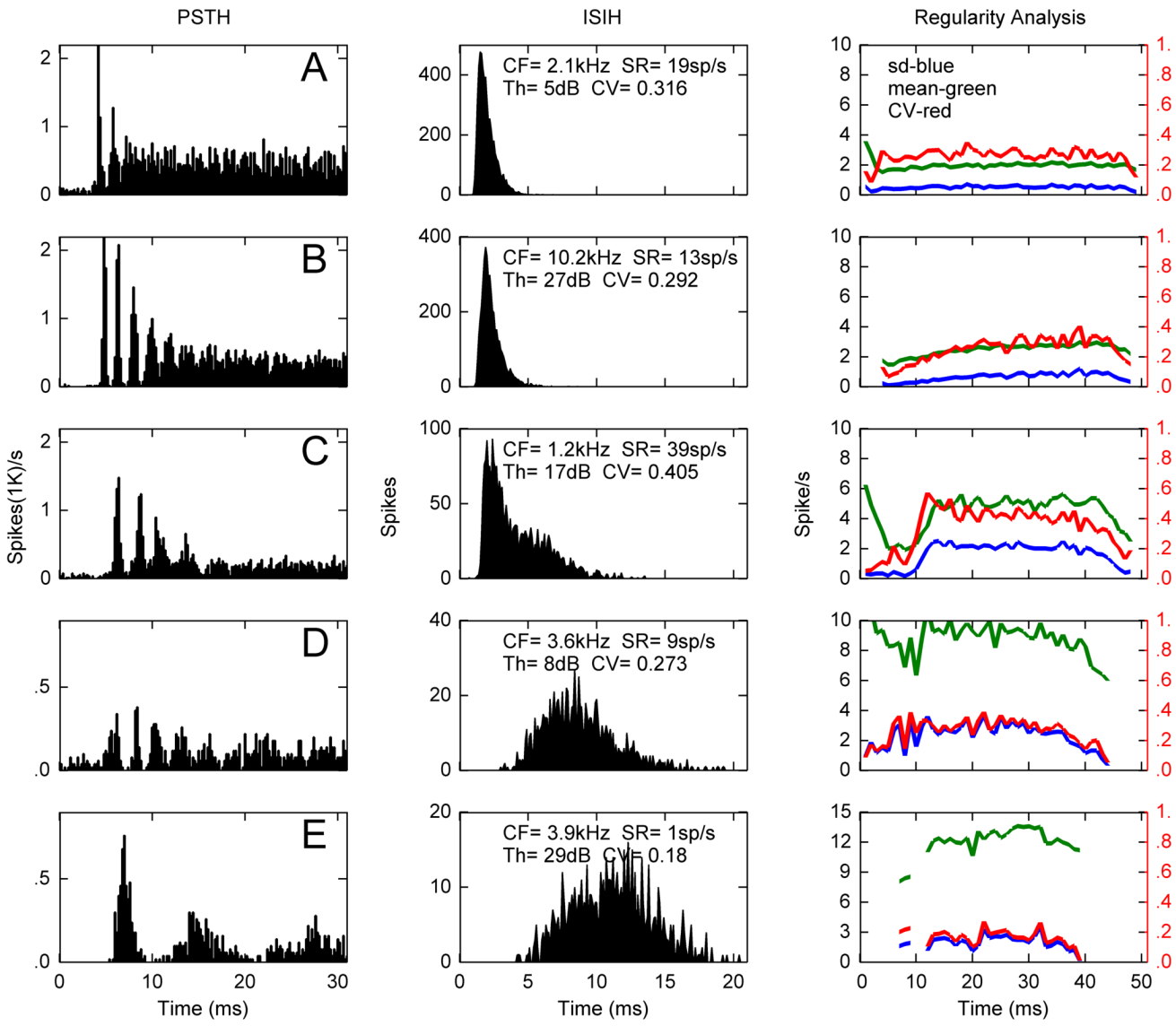

Figure 4.

Post stimulus time (left) and interspike interval (right) histograms from four Ct (A–D) and one Cw (E) units in the squirrel monkey and marmoset (A). Characteristic frequency, spontaneous rate, threshold and coefficient of variation for the ISIH are indicated for each unit. Regularity analysis in column 3 shows the mean interspike-interval (green), its standard deviation (blue) and CV (red). The drop off after 40 ms is an edge effect due to the termination of the stimulus at 50 ms.

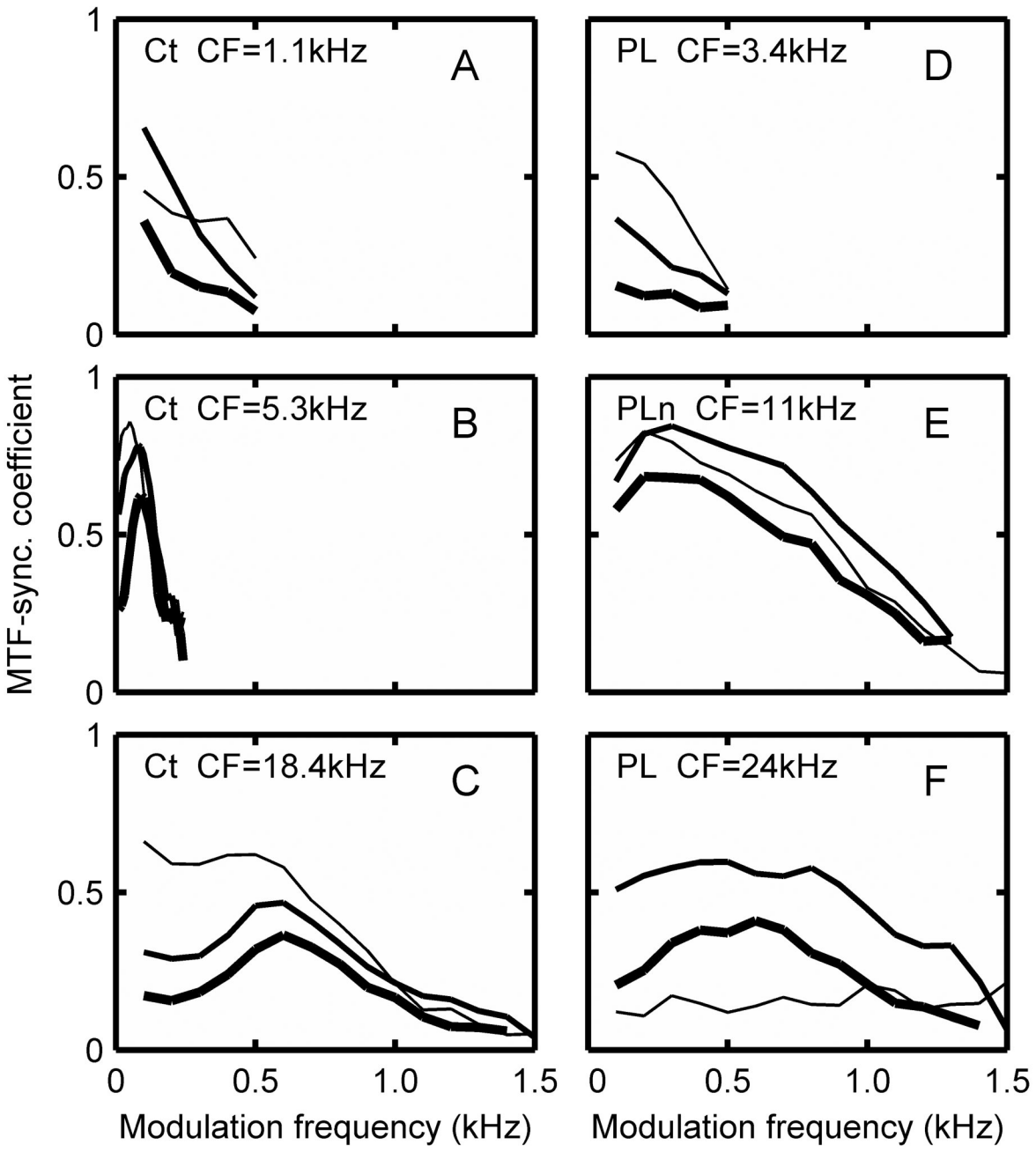

Figure 5.
Modulation transfer function synchronization coefficients of 3 example Ct (A–C), 2 PL (D, F), and PLn (E) neurons at 30 dB (thin line), 50dB (medium line), and 70dB (heavy line) plotted as a function of AM modulation frequency. CFs of individual cells are indicated. 2 squirrel monkey and 4 marmoset neurons were used for the example units.

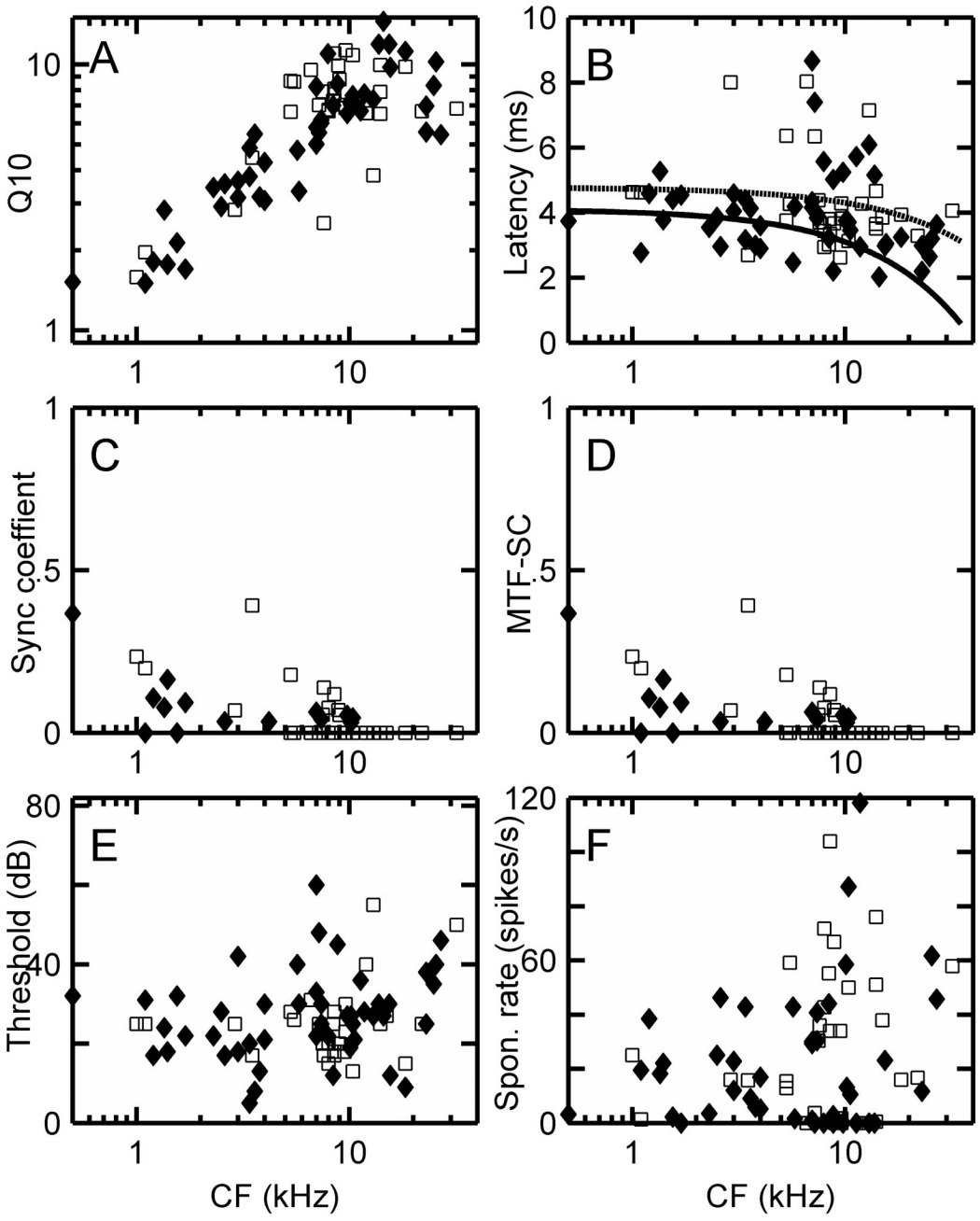

Figure 6.

(A) Q10 = CF/bandwidth at 10 dB above threshold on a log-log scale, (B) latency, (C) maximum synchronization coefficient from the PSTH at CF, (D) maximum MTF synchronization coefficient, (E) thresholds in dB, and (F) spontaneous rates in spikes/s for Ct units in the squirrel monkey (♦) and marmoset (□). The MTF-SC is the maximum value observed over the range of AM modulation frequencies (typically 50 – 2550 Hz) used for each unit. Regression lines were fitted to squirrel monkey (solid line) and marmoset (dashed line) latency data (B), and four outliers with latencies exceeding 8 ms were excluded from the fits.

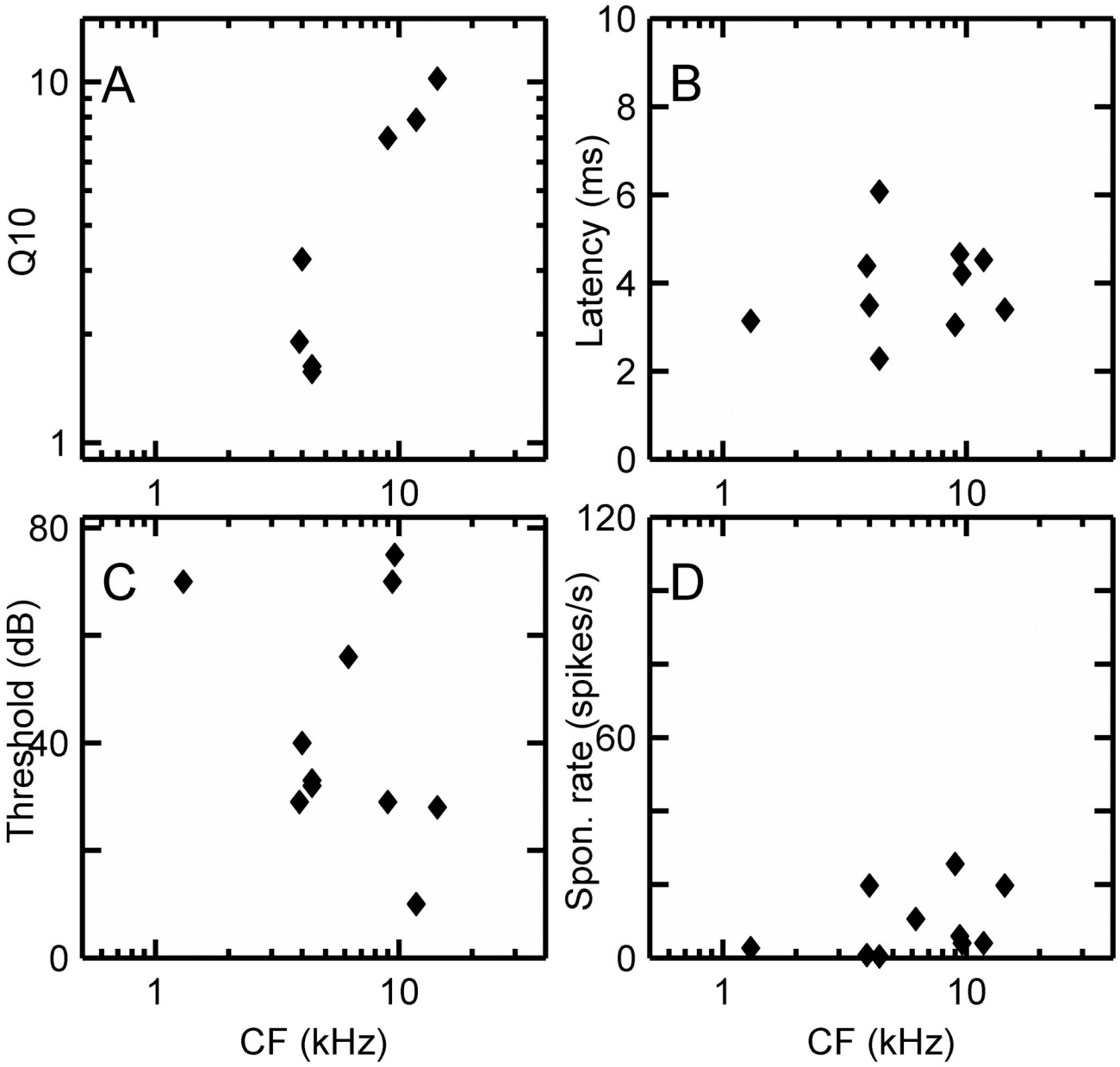

Figure 7.
(A) Q10, (B) latency, (C) threshold, and (D) spontaneous rate data for low discharge rate Cw units in the squirrel monkey.

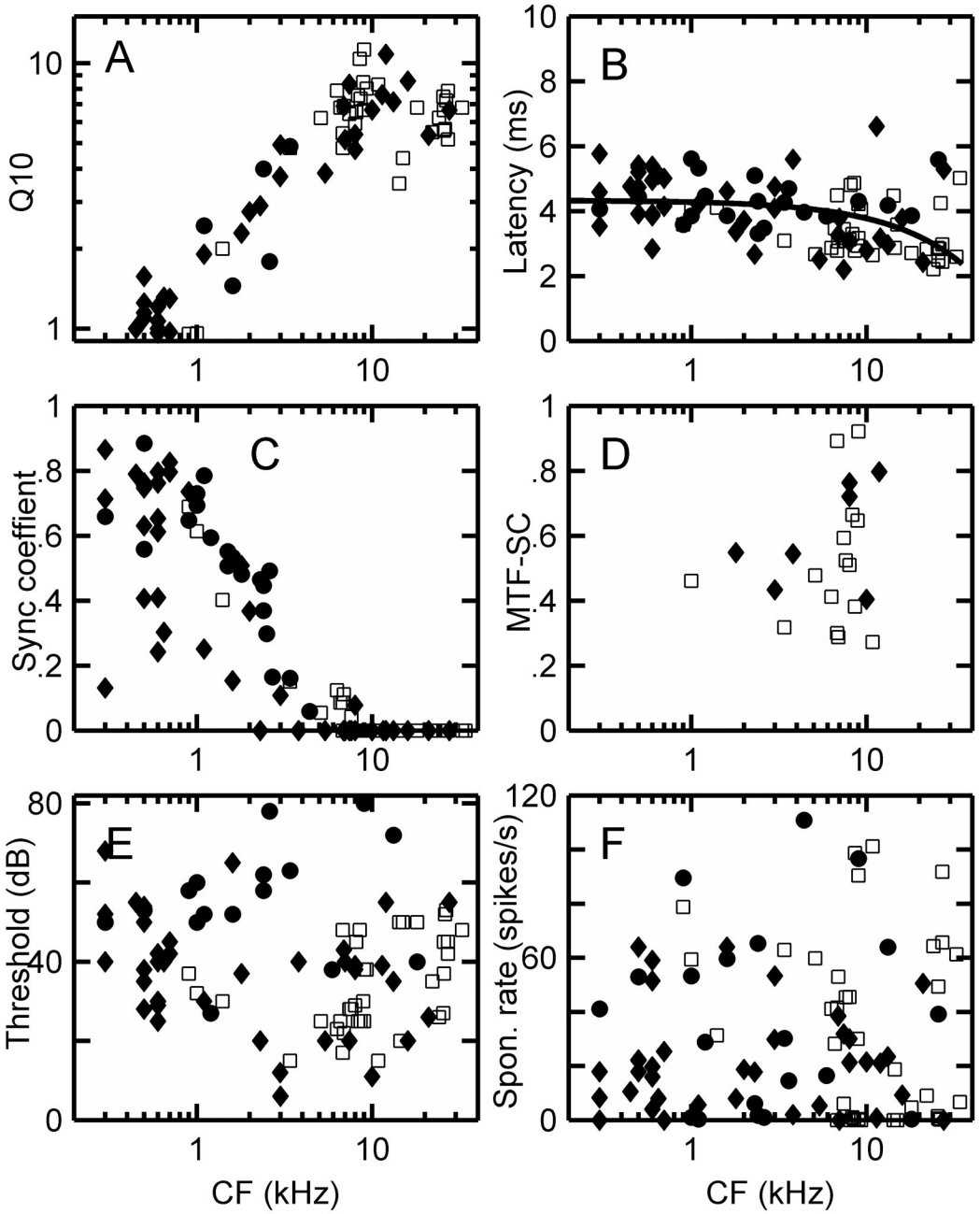

Figure 8.

(A) Q10, (B) latency, (C) synchronization coefficient from PSTH at CF, (D) maximum MTF synchronization coefficient values, (E) thresholds in dB, and (F) spontaneous rates in spikes/s for PL units in the squirrel monkey (♦), cynomolgus macaque (●), and marmoset (□). A regression line has been fitted to the combined latency data from all species in (B).

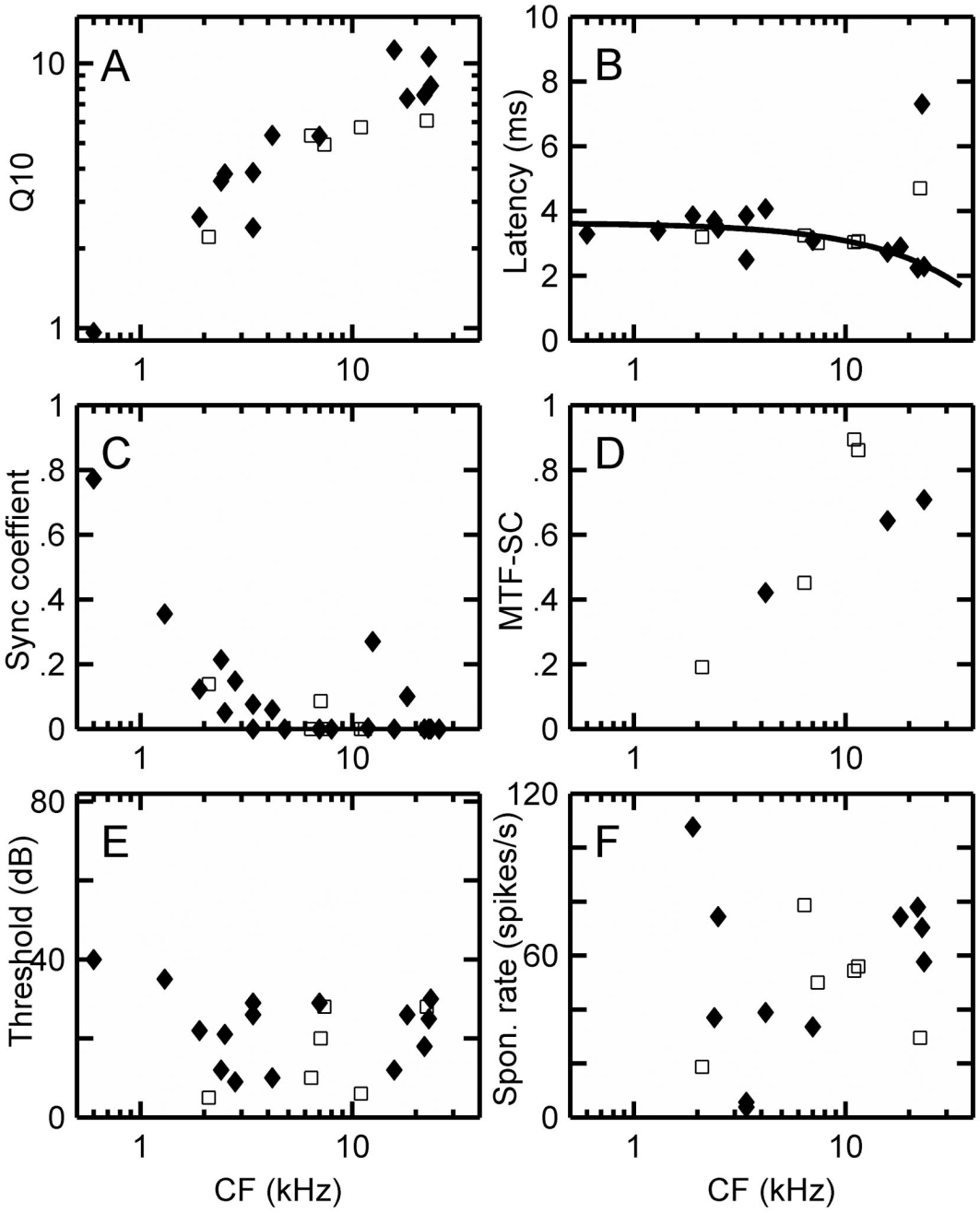

Figure 9.

(A) Q10, (B) latency, (C) synchronization coefficient, (D) maximum synchronization coefficient from MTF, (E) thresholds in dB, and (F) spontaneous rates in spikes/s for PLn units in the squirrel monkey (♦) and marmoset (□). Only 4 MTFs were recorded from PLn units in these species, and those values are included for completeness. A regression line has been fitted to the combined latency values for both species in B, and two outliers with CFs just above 20 kHz were excluded from the fit.

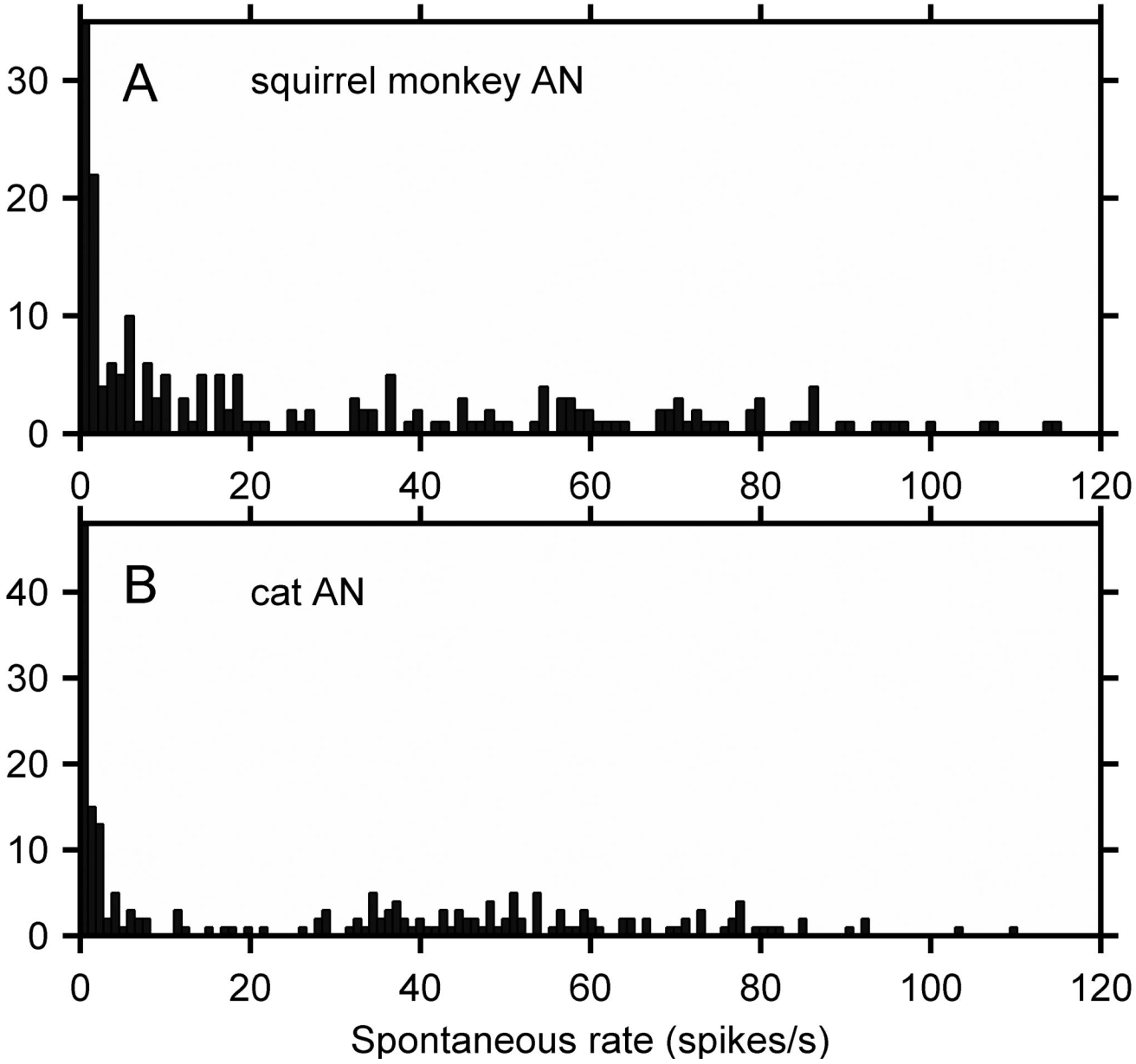

Figure 10.
(A) Spontaneous rates of squirrel monkey VIIIth nerve fibers (N=218) taken from Geisler et al. (1974). (B) For comparison, spontaneous rates of cat VIIIth nerve fibers (N=203) taken from Rhode and Smith (1985) and Rhode and Greenberg (1997).

Table 1

The number of units of each response type in each monkey sub-species (number of subjects) and the percentage each response type represents for all species combined. Response types typically associated with the DCN (i.e. P/C, PBC, B, and Types 2, IV, and IV) are combined as "All others," but P units are separated because 10 units were studied. Note these data do not constitute random samples of the CN complex from the three primate species.

PSTH	MM (1)	Cyno (3)	SM (7)	Total	% Total
Cw	3	3	11	17	5.7%
Ct	32	1	51	84	28.4%
Cs	1	0	4	5	1.7%
On	2	5	5	12	4.1%
OnC	0	6	8	14	4.7%
OnI	0	0	4	4	1.4%
PL	37	27	44	108	36.5%
PLn	7	3	20	30	10.1%
P	4	2	4	10	3.4%
All others	3	1	6	12	4.0%
Total classified				296	100%
Total recorded				373	

Table 2

Mean and (SD) of several descriptive statistics for 3 response types of marmoset CN neurons. The number of units of each response type is shown (top row). Mean and standard deviation reported for each was typically done on a subpopulation of the N in each group. A blank is shown if no data or insufficient data were recorded for that particular parameter, and no SDs are reported for response categories or response parameters with less than 5 data points. PST-SC* values are the synchronization coefficients (SC) obtained from the PSTH response at CF (250 repetitions with values shown only for those neurons with CFs ≤ 2 kHz (i.e. 2 Ct and 3 PL units). MTF-SC values are the highest SCs obtained from the temporal modulation transfer functions.

Parameter	CT (32)	PL (37)	PLn (7)
SR (spikes/s)	32.4 (30.3)	33.8 (33.3)	47.0 (21.2)
TH (dB)	25.1 (9.3)	34.1 (11.5)	16.2 (10.6)
DR (dB)	34.8 (14.3)	31.7 (9.6)	27.5 (8.7)
PST-SC*	0.22	0.57	
MTF-SC	0.67 (0.14)	0.69 (0.14)	

Table 3

Mean and (SD) of several descriptive statistics for 6 response types of squirrel monkey CN neurons. As described in methods, the number of each response type encountered is shown, and the mean and standard deviation reported for each was typically done on a subpopulation of the N in each group. A blank is shown if no data or insufficient data were available for that particular parameter. PST SC* values are shown only for those neurons with CF $\leq$ 2 kHz.

Parameter	Cw (11)	Ct (51)	On (5)	OnC (8)	PL (44)	PLn (20)
SR (Spikes/s)	8.5 (9.1)	36.8 (50.9)	4.3 (3.5)	7.3 (6.6)	22.7 (19.8)	75.2 (53.1)
TH (dB)	42.9 (21.4)	27.4 (11.3)	32.3 (14.9)	44.6 (23.3)	36.9 (14.3)	23.9 (8.8)
DR (dB)	35.7 (22.1)	28.4 (13.4)	32.5 (19.4)	45.0 (18.0)	29.0 (11.2)	23.6 (16.4)
PST-SC*		0.12 (0.13)		0.09	0.57 (0.24)	0.42
MTF-SC	0.68	0.65 (0.13)		0.81	0.63 (0.16)	0.58

Table 4

Summary spontaneous rate, threshold, and synchronization coefficient values from PST histograms and MTFs as derived from squirrel monkeys and marmosets. Threshold values exclude 3 Cw, 2 OnC, and 2 PL units in the squirrel monkey with thresholds ≥ 65 dB. PST SC* values were only calculated for units with CFs <= 2 kHz

Response type (#)	SR (spikes/s) (SD)	Threshold (dB) (SD)	PSTH-SC (SD)	MTF-SC (SD)
Cw (14)	14.0 (16.3)	30.2 (11.5)		0.67 (0.15)
Ct(84)	38.8 (50.9)	26.5 (10.5)	0.14 (0.12)	0.65 (0.13)
On(5)	4.3 (3.5)	35.7 (12.8)		0.84
OnC(8)	7.3 (6.6)	32.4 (12.3)		0.81
P(10)	21.9 (24.8)	21.1 (12.6)		0.74
PL(81)	27.8 (26.0)	34.7 (12.1)	0.59 (0.20)	0.61 (0.14)
PLn(30)	64.4 (47.4)	21.6 (9.8)		0.64 (0.20)

Table 5

Primate auditory-nerve fiber spontaneous rate data from published and unpublished data.

SR(spikes/s)	Nomoto et al.	Geisler et al.	Rose et al.
0–10	35.9%	47.7%	23%
11–51	30.8%	23.9%	37%
51–110	33.3%	28.4%	40%